Report
R-17-20
December 2017

Thermodynamic evaluation of impurity elements in OFP copper

Hans Magnusson

SVENSK KÄRNBRÄNSLEHANTERING AB

SWEDISH NUCLEAR FUEL
AND WASTE MANAGEMENT CO

Box 3091, SE-169 03 Solna
Phone +46 8 459 84 00
skb.se

SVENSK KÄRNBRÄNSLEHANTERING

ISSN 1402-3091
SKB R-17-20
ID 1594083
December 2017

Thermodynamic evaluation of impurity elements in OFP copper

Hans Magnusson, Swerea KIMAB AB

Abstract

Many polycrystalline copper grades show a loss in ductility around 200 °C due to intergranular fracture characterised by voiding and fracture at grain boundaries. This ductility loss can be related to the alloying content of the copper material. This is true also for the impurity elements in copper which are often present in low concentrations. It has been demonstrated in the literature that most of the ductility loss can be avoided by going from OFHC-copper (99.95 % Cu) to high purity coppers (higher than 99.9999 %). The importance of alloying elements and impurities in coppers, and the difficulty in experimentally finding these low concentrations of elements in the microstructure, motivates a computational study to highlight the most likely reactions taking place between alloying and impurity elements in copper. Special interest in this work is to investigate if phosphorus will influence the impurity elements in copper.

Thermodynamic calculations have been made at room temperature according to the ternary copper-phosphate-impurity system Cu-P-X. The studied impurities in this work are: Pb, Zn, Fe, Ag, As, Sb, Te, Bi, Cd, Mn, Ni, Se, Sn, O and S. The results from the calculations can be summarised as:

- Impurity occurring in solid solution: As, Zn, Mn, Sb, Sn, Cd, and P.
- Impurity precipitate occurring as inclusion, not containing copper: Pb, Bi, B, and Ag.
- Impurity precipitate occurring as inclusion with copper: Hg, Se, Te, and S.
- Impurity precipitate occurring as phosphorus compound: O (phosphate), Fe, and Ni (phosphides).

The results from thermodynamic calculations have been compared to data of embrittling elements of copper, such as bismuth, tellurium, lead, selenium and sulphur. The calculations indicate that all these elements have a low solubility in copper and will precipitate. Phosphorus will not influence these reactions.

Of all studied elements, the only elements that do show an influence of phosphorus are oxygen, nickel and iron. The phosphorus-oxygen interactions have been evaluated in a previous work, which showed that copper phosphates are more stable than copper oxides. Both iron and nickel are expected to react with phosphorus forming phosphides. These two elements form phosphides with similar crystalline structure and can substitute each other. The iron phosphide has higher stability than the nickel variant, and is expected to be the most important one.

Sammanfattning

Koppar som metall uppvisar ofta en god duktilitet med stor töjning till brott vid provning. Ett undantag är vid temperaturer runt 200 °C där kommersiella kopparlegeringar ofta visar försämrad duktilitet. Vid dessa temperaturer sker intergranulärt brott genom sprickpropagering i korngränser. Detta fenomen har tidigare i litteraturen relaterats till renheten av kopparmaterialet. Genom att gå från exempelvis OFHC-koppar med 99,95 % koppar till högren koppar med 99,9999 % koppar kan man undvika det mesta av denna duktilitetsförsämring.

Syftet med denna studie är därför att undersöka vilka tänkbara kemiska reaktioner som kan ske mellan spårelement, fosfor och koppar i OFP-koppar. De låga koncentrationerna av spårelement i OFP-koppar gör experimentell karakterisering besvärlig, vilket motiverar beräkningar för att öka förståelsen runt förväntade reaktioner i materialet.

Termodynamisk utvärdering har genomförts för ett stort antal legeringssystem som baseras på koppar och fosfor, samt ytterligare ett legeringselement enligt Cu-P-X, där X är något av elementen: Pb, Zn, Fe, Ag, As, Sb, Te, Bi, Cd, Mn, Ni, Se, Sn, O och S. De förväntade reaktionerna kan sammanfattas enligt:

- Spårelement förväntas kvarstå i lösning i kopparmatrisen: As, Zn, Mn, Sb, Sn, Cd och P.
- Spårelement utskiljs som inneslutning utan koppar: Pb, Bi, B och Ag.
- Spårelement utskiljs som inneslutning med koppar: Hg, Se, Te och S.
- Spårelement utskiljs med fosfor: O (fosfat), Fe och Ni (fosfider).

Ovanstående resultat från den termodynamiska analysen har jämförts med experimentella observationer gällande spårelementens inverkan på duktiliteten av koppar. Överlag kan man se en tydlig koppling mellan utskiljande element samt element som verkar förspödande. Dock finns ingen tydlig indikation på hur fosfor kan påverka dessa reaktioner.

De spårelement som kan reagera med fosfor är syre, järn och nickel. Stabiliteten av fosfater har diskuterats i ett tidigare arbete, där det påvisades att fosfater är mer stabila än kopparoxider. Både järn och nickel förväntas bilda fosfider, av liknande kristallstrukturer. Järnfosfiden har i regel en högre stabilitet än motsvarande nickelfosfid.

Contents

1 Introduction

Oxygen-free phosphorus copper (OFP copper) is suggested as canister material for disposal of spent nuclear fuel in Sweden. The material is nearly pure copper and the only added alloying element is phosphorus in concentration 30–100 wtppm. The specifications for OFP copper follow a material standard for oxygen-free high conductivity coppers (OFHC-copper), C10100. This standard specifies the maximum concentration of impurity elements that are allowed in these coppers at production. Some additional limits have been given according to the application, that sulphur should be less than 12 wtppm, hydrogen less than 0.6 wtppm, and oxygen in copper ingots less than 5 wtppm (SKB 2010).

Many polycrystalline copper grades often show a loss in ductility around 200 °C (Laporte and Mortensen 2009). This is believed to be due to intergranular fracture characterised by voiding and fracture at grain boundaries. It has been shown experimentally, that by alloying with phosphorus both the creep strength and ductility improves at low temperature testing (Andersson-Östling and Sandström 2009). This effect is seen already for low concentrations of phosphorus. Grain boundary regions only occupy a minor part of the material and this could explain why only ppm level of phosphorus is needed to improve creep properties.

Attempts have been made to explain the positive effect of phosphorus in copper. Due to the type of intergranular fracture, the positive influence of phosphorus has been attributed to enrichments of phosphorus at the boundaries and thus influences the ductility of OFP copper (Sandström and Wu 2013). However, it is difficult to verify these theories due to the low concentration of phosphorus in the material. Some attempts have been made previously to measure phosphorus, for instance atom probe measurements made by Thuvander (2015), who indicated a quite homogeneous phosphorus distribution in the Cu lattice. No phosphides were found in this study. Measurements by Andersson-Östling et al. (2017) have shown similar results with a homogeneous phosphorus distribution in the Cu lattice.

The purity of copper alloys will directly influence the ductility loss. Fujiwara and Abiko (1995) have shown that most of the ductility loss of coppers was avoided by going from 3N5 OFHC-copper (99.95 % copper) to higher purity 6N (99.9999 % Cu) and 8N coppers (99.999999 % Cu). This finding demonstrates that minor concentrations of impurities will influence the properties of copper alloys. An interesting hypothesis to evaluate is if phosphorus could influence the chemical reactions of these impurities in OFP coppers, and explain the improved mechanical properties due to phosphorus alloying.

Due to the low concentrations of phosphorus, and the even lower concentrations of impurity elements, the possible precipitates will be few in number. It is therefore of interest to evaluate the possible reactions that can occur with phosphorus in OFP copper by computational methods. In a previous work, phase equilibria for the Cu-H-O-S-P system have been evaluated (Magnusson and Frisk 2013). Special interest in this study is to evaluate the possible reactions between phosphorus and other impurity element. The following topics will be studied in this work:

- Solubility of impurity element in copper.
- Possible phases including impurity elements and copper.
- Solubility of impurity element in copper in the presence of phosphorus.
- Possible phosphides including impurity elements in copper.

A limitation in this work is that the influence of an impurity element in copper is limited to its ternary system according to Cu-P-X. This implies that any reaction between two different impurity elements in copper is not considered. However, since the phosphorus-impurity reactions are of greatest interest in order to explain the influence of phosphorus, this limitation is accepted.

2 Material and methods

2.1 OFP copper and its specifications according to standard

The concentration of impurity elements according to the material standard C10100 is given in Table 2-1. Most of the impurity elements are specified to be below 5 wtppm in concentration, except iron 10 wtppm, nickel 10 wtppm, and silver 25 wtppm. Hydrogen, oxygen and sulphur have been studied in a previous work (Magnusson and Frisk 2013).

Table 2-1. Compositional limits according to C10100 standard. Concentrations are given in weight-percent and wtppm.

Cu	Pb	Zn	Fe	P	Ag	As	O	Sb
99.99	0.0005 5 ppm	0.0001 1 ppm	0.001 10 ppm	0.0003 3 ppm	0.0025 25 ppm	0.0005 5 ppm	0.0005 5 ppm	0.004 4 ppm
	Te	**Bi**	**Cd**	**Mn**	**Ni**	**Se**	**S**	**Sn**
	0.0002 2 ppm	0.0001 1 ppm	0.0001 1 ppm	0.00005 0.5 ppm	0.001 10 ppm	0.0003 3 ppm	0.0015 15 ppm	0.0002 2 ppm

2.2 Thermodynamic calculations

In order to answer if the impurity element will remain in solid solution, or react with copper or phosphorus, a thermodynamic evaluation will be made. Some alloying systems have been studied more than others and the approach to get information needed for the thermodynamic calculation will vary. The more studied systems have been evaluated by computational thermodynamics following the CALPHAD approach. This approach ensures a critical assessment of the alloy systems based on experimental phase diagram and thermochemical information (Saunders and Miodownik 1998, Lukas et al. 2007). Some of these systems have been assessed many times allowing for refinements over time typically due to additional experimental data or new areas of interest. It is likely that reliable calculations for impurities in OFP copper can be made for these systems.

Binary evaluations following the CALPHAD method are based on the same referencing system, i.e. the same Gibbs energy expressions of pure elements. This common reference plane allows for combining different lower ordered systems such as binaries to make extrapolations for higher-ordered systems like ternaries. This step enables equilibrium calculations of impurity element in phosphorus alloyed copper. For instance, the Cu-P evaluation by Noda et al. (2009) can be combined with a copper-impurity system Cu-X, and phosphorus-impurity system P-X giving the ternary system Cu-P-X.

It is more difficult to get the needed information from those alloying systems that have not been assessed by computational thermodynamics. For some of these systems, experimental reviews are available which can give an indication of the phase equilibria. These reviews can show if the impurity elements should remain in solid solution or precipitate as an inclusion. The phase diagrams are often hand-drawn based on the gathered experimental data. The main limitation with these evaluations is that they cannot be used for extrapolation to higher ordered systems, and that it is not possible to calculate equilibria of the impurity element in phosphorus alloyed copper.

For some alloying systems which are of less commercial or scientific interest, little thermodynamic data is available. Some observations might exist for a limited part of the alloying system. Making calculations for these systems is challenging. Sometimes data can be found in different thermo-chemical handbooks, which tabulates Gibbs energy of formation for stoichiometric compounds. By tradition, the Gibbs energy of these compounds is stated at 298.15K relative to the pure elements in their reference phase. This data is useful and can be used to calculate equilibria at 298.15K. Calculations at any higher temperature will not be possible, since it requires additional thermo-chemical data which is not always available. A low temperature, such as 298.15K, is of interest for

the canister material in service. It should be noted that the kinetics including element diffusion is limited at these temperatures, but can to some extent be compensated by the long service life of the canister material.

For all impurities, the aim is to have a thermodynamic description of the Cu-P-X system, where X is the impurity element. In order to assess this, the Cu-X system will first be evaluated. This binary gives information of the solubility of the impurity in copper as well as copper-impurity compounds. The second task is to check the P-X binary system, giving information on what phosphides can be expected and their stability. Finally, the Cu-X, P-X and Cu-P binaries are all combined giving the ternary Cu-P-X system. Based on this ternary system, thermodynamic calculations are made at room temperature 298.15K. A phosphorus content of 50 wtppm will be used in the calculations. The concentration of impurity will be taken as its maximum level according to standards (Table 2-1).

2.3 Embrittling elements in copper

Embrittlement of copper alloys has been reviewed by Laporte and Mortensen (2009), who have summarised the effect of many different alloying elements on the ductility of copper alloys. It should be noted that in their study they summarise experimental findings based on experiments that often uses much higher concentrations of impurities than what is of interest in this work. In addition, the alloys are not often of controlled impurity and other elements might influence as well. Nevertheless, their work will be used as a reference on the ductility loss in copper due to impurity elements and compared with the findings from the thermodynamic evaluation.

An additional report by Gavin et al. (1978) will be used as reference on copper ductility. Gavin et al. rank the most potent embrittlement elements of copper as: Bi, Te, Pb, Se, and S. Laporte and Mortensen (2009) adds some elements to this list: Sn, O, Sb, and to some extent P. A reverse de-embrittling effect has been reported for some elements, for instance B, Mn and P. Phosphorus shows a double appearance, and its effect will depend on the purity and type of alloy. Laporte and Mortensen refer to Ozgowicz and Biscondi (1995) for a negative effect of phosphorus on tin-bronzes. For similar tin-bronzes, Kanno et al. (1987) have reported a minor positive influence of phosphorus. The influence of phosphorus for these highly alloyed copper materials seems minor and their effect on ppm-levels of phosphorus in OFP copper cannot be concluded from these findings. These limitations should be taken into consideration when comparing the embrittling effect of impurities with thermodynamic calculations.

3 Summary of results from thermodynamic evaluation

3.1 Presentation of results

All thermodynamic evaluations for Cu-X systems are presented in Section A1. The corresponding P-X systems and the combined ternary Cu-P-X systems are presented in Section A2. The findings from these evaluations is summarised here. To start with, the availability of literature data needed for the calculations is summarised in Section 3.2. Then, the results from thermodynamic calculations for all Cu-P-X systems is summarised in Section 3.3, and compared with reported data on the embrittling effect of impurities in Section 3.4.

3.2 Available data for evaluation

Status for the literature survey is summarised in Table 3-1. This table indicates the data that has been used when making calculation for the impurity element in OFP copper according to its Cu-P-X system. The green colour is used for those alloying system which have been assessed by computational thermodynamics and accepted in this evaluation. It can be seen that most of the Cu-binaries have available descriptions in the literature, with Cu-Te as the only exception. For this system an experimental evaluation is available and indicates that this system behaves as the related systems Cu-S and Cu-Se, with a very low solubility in metallic copper and precipitates of Cu_2X type. For this reason all Cu-X binaries are considered as well studied in this work.

The phosphorus binaries P-X are not as well studied as the copper binaries. Some of the system with relation to commercially important systems have been studied, like bronze (Sn), steels (Fe, Mn, Ni), and semiconductor materials (As). For the remaining systems no computational based thermodynamic assessment has been found in the literature. Some of these systems have experimental reviews available, which are marked as yellow. These experimental reviews give a good overview of the alloying system, but they cannot be used directly to make calculations for the ternary system. For some of the P-X binaries, no computational or experimental reviews are available, marked as orange. Not much data has been published, although in some cases thermochemical data is available which makes it possible to make estimates for the ternary system.

Compounds between an impurity element and phosphorus will in this work be denoted as phosphides. For most of the metallic elements this is the natural designation, but for some of the lighter elements this might not be the correct spelling. However, in order to simplify the comparison between different phosphorus compounds in various alloying systems this designation will be used.

3.3 Equilibrium calculations for impurity element in OFP copper

Equilibrium calculations have been made at 298.15K using 50 wtppm of phosphorus and maximum level of impurity according to the C10100 standard (Table 2-1). Two elements included in this work, boron and mercury, are not specified in the standard. However, it can be noted that the solubility of these elements in copper is very low and below 1 wtppm.

Table 3-2 summarise the findings from all evaluations. The second column in Table 3-2 indicates if the impurity element is completely in solution according to the Cu-X binary. According to this list quite few impurities elements will completely remain in solid solution. These impurities are arsenic, zinc, manganese, nickel, and tin. Some additional elements are expected to remain in solid solution but are close to their solubility limit. These are antimony, cadmium and phosphorus. The remaining impurities will reach their solubility limits and precipitate in some form. Some of these elements precipitate as separate inclusions not including copper, such as iron, lead, bismuth, boron and silver. The other will precipitate with copper on Cu_2X stoichiometry, which is mainly the chalcogen elements oxygen, sulphur, selenium and tellurium.

Table 3-1. Status of literature review in this work. Green colour indicate that a thermodynamic evaluation has been found. Yellow means that no thermodynamic assessment has been found, but experimental data is available and allows for conclusions about impact. Orange means that observations are available that phosphides exists, but not sufficient thermodynamic data for including them in calculation.

Impurity	Cu-X binary	P-X binary	Cu-P-X ternary
As	Uhland et al. (2001)	Ansara et al. (1994)	From binaries
Zn	Liang et al. (2015)	Experimental evaluation exists but no reliable computational assessment. Thermochemical data reported for Zn_3P_2 and ZnP_2.	From Cu-P, Cu-Zn, and reported Gibbs energy for phosphides at 298.15K.
Mn	Miettinen (2003)	Miettinen and Vassilev (2014c)	From binaries
Fe	Chen and Jin (1995)	Miettinen and Vassilev (2014a).	From binaries
Ni	An Mey (1992)	Miettinen and Vassilev (2015)	From binaries
Sb	Liu et al. (2000)	Ansara et al. (1994)	From binaries
Sn	Wang et al. (2011)	Hino et al. (2011)	From binaries
Pb	Teppo et al. (1991)	No assessment or experimental evaluation of system. One phosphide has been reported, Pb_6P but no thermochemical data.	From Cu-P, and Cu-Pb binaries. No data for lead phosphide.
Bi	Teppo et al. (1990)	No assessment or experimental evaluation of system. One phosphide has been reported BiP	From Cu-P, and Cu-Bi binaries. No data for bismuth phosphide.
B	Wang et al. (2009)	No assessment or experimental evaluation of system. $B_{13}P_2$ and BP reported stable phosphides. Thermochemical data available.	From Cu-P, and Cu-B binaries plus reported Gibbs energies at 298.15K for both phosphides.
Ag	Moon et al. (2000)	Experimental evaluations exists of both binary and ternary system, but no assessment. AgP_2 and AgP_3 phosphides are stable, and thermochemical data reported.	From Cu-P, and Cu-Ag binaries plus reported Gibbs energies at 298.15K for both phosphides.
Cd	Chen et al. (2010)	No assessment or experimental evaluation of system exists. Cd_3P_2 and CdP_2 phosphides have been reported. Thermochemical data for Cd_3P_2.	From Cu-P, and Cu-Cd binaries plus reported Gibbs energies for Cd_3P_2 at 298.15K
Hg	Liu et al. (2012)	No assessment, but experimental review of system exists. No mercury phosphide reported.	From Cu-P and Cu-Hg binaries.
Se	Du et al. (2008)	No assessment, but experimental review exists. P_4Se_4, P_4Se_3, and P_4Se_5 phosphides are stable. No thermochemical data available.	From binaries Cu-P, and Cu-Se. No data for selenium phosphides.
Te	No thermodynamic assessment, but available experimental evaluations	No assessment, but experimental review exists. PTe is reported stable phosphide. No thermochemical data available.	No calculations made for ternary system.

Column three in Table 3-2 summarises the 28 different phosphides that have been included in this evaluation. Some additional phosphides have been reported in the literature, but these have not been included in calculations due to lack of thermochemical data. These are 7 phosphides containing lead, bismuth, cadmium, selenium and tellurium. Selenium and tellurium reacts strongly with copper forming copper compounds, in similarity with sulphur in copper. Sulphur phosphides exists but these are never close to become stable (Magnusson and Frisk 2013), and a similar relation should hold for selenium and tellurium in phosphorus containing copper. Lead, bismuth and cadmium are all low-melting elements and their phosphides should have low stability as well. Phosphides will

practically never precipitate and grow at low-temperature due to the very slow diffusion of elements in copper at these temperatures. For these reasons, it is believed that these phosphides should not be of any greater importance for OFP copper, but this cannot be shown in this work by thermodynamic calculations due to lack of data.

The fourth column in Table 3-2 indicates if any of the phosphides listed in the third column are likely to become stable in OFP copper. This column summarise the results from equilibrium calculations for the Cu-P-X system. It can be seen that in nearly all cases a phosphide including the impurity element will not become stable. Only iron, nickel and oxygen are expected to precipitate with phosphorus. These three elements will be further discussed in Section 3.5.

Table 3-2. Evaluated solubility of impurity in copper, according to standard (Table 2-1). The number of phosphides considered is noted and if they are likely to become stable in OFP copper is indicated as well. Green indicates that the elements is in solution, yellow in solution but close to solubility limit, and orange indicates precipitation of impurity.

Impurity	Position of impurity element according to Cu-X binary	Phosphides included in ternary description	Is phosphide likely to become stable for Cu-P-X?
As	Yes	AsP	No
Zn	Yes	Zn_3P_2, ZnP_2	No
Mn	Yes	Mn_3P, Mn_2P, MnP	No
Fe	No, alfa-Fe *Im$\bar{3}$m*	Fe_3P, Fe_2P, FeP, FeP_2, FeP_4	Yes, FeP_2
Ni	Yes	Ni_3P, Ni_5P_2, $Ni_{12}P_5$, Ni_2P	Yes, Ni_2P
Sb	Yes, close to limit, Cu_4Sb (δ-phase), *$P6_3/mmc$*	None included	No
Sn	Yes	Sn_4P_3, Sn_3P_4, SnP_3	No
Pb	No, Pb-phase *Fm$\bar{3}$m*	None included (Pb_6P reported)	Not likely
Bi	No, Bi-phase, *R$\bar{3}$m*	None included (BiP reported)	Not likely
B	No, B-phase, *R$\bar{3}$m*	BP, $B_{13}P_2$	No
Ag	No, Ag-phase *Fm$\bar{3}$m*, close to solubility limit	AgP_2, AgP_3	No
Cd	Yes, close to limit, $CdCu_2$, *$P6_3/mmc$*	Cd_3P_2 (CdP_2 also reported)	Not likely
Hg	No, Cu_7Hg_6, *R$\bar{3}$m*	None included	No
Se	No, Cu_2Se, *Fm$\bar{3}$m* (β)	None included (Se_3P_4, Se_4P_4, Se_5P_4 reported)	Not likely
Te	No, Cu_2Te	None included (TeP reported)	Not likely
O	No, Cu_2O, *Pn$\bar{3}$m*	P_2O_5, $Cu_2P_2O_7$, and $Cu_3(PO_4)_2$.	Phosphates $Cu_3(PO_4)_2$, or $Cu_2P_2O_7$
S	No, Cu_2S, *Fm$\bar{3}$m*, Digenite	P_4S_5, P_4S_7, P_4S_{10}, and P_4S_3	No
P	Yes, but close to limit Cu_3P, *$P6_3$ cm*	–	–

3.4 Comparing thermodynamic calculations with reported embrittlement

The thermodynamic review of the Cu-P-X impurity systems gave information on possible chemical reactions that can occur between impurity and phosphorus in copper. These findings are summarised in Table 3-3, and compared with data on reported embrittlement effects of impurities in copper according to Gavin et al. (1978) and Laporte and Mortensen (2009).

Gavin et al. (1978) indicated that the most important elements that control the ductility of copper are bismuth, tellurium, lead, selenium, and sulphur. All these elements are expected to precipitate in copper according to the thermodynamic review made in this work. It is noted that phosphorus is not expected to have any significant influence on phase equilbria for these impurities.

Laporte and Mortensen (2009) added some additional elements as important for copper ductility. In similarity with the other chalcogen elements sulphur, selenium and tellurium, also oxygen is expected to lower the ductility of coppers. The oxygen-phosphorus reaction is strong, and phosphates are expected to be more stable than copper oxide (Magnusson and Frisk 2013). Oxygen is one of few elements were phosphorus will have an influence on phase stability. The other two elements are iron and nickel which will be discussed in next chapter.

The review by Laporte and Mortensen (2009) relied on copper alloys with high concentrations of impurities. For this reason their findings cannot easily be applied for OFP copper that contains ppm levels of impurities. One example is for tin, which was based on data for bronze alloys which showed that tin can lower the ductility of copper at low temperature for Cu-8Sn alloys (Barrera et al. 1992). Although tin has a high solubility in copper at high temperatures, it falls rapidly with temperature and could precipitate at low temperatures in these concentrations. On the other hand, ppm levels of tin are expected to remain in solid solution with little influence on ductility.

Table 3-3. The expected position of the impurity element in lattice according to thermodynamic evaluation. This data is compared with reported embrittling due to impurity element according to Laporte and Mortensen (2009), and Gavin et al. (1978). Green indicate that the impurity remains in solid solution, yellow is the same but it is close to solubility limit, orange is impurity precipitation together with phosphorus and pink is precipitates without any influence of phosphorus.

Impurity	Impurity position according to ternary	Reported embrittling element in copper	
		Laporte and Mortensen (2009)	Gavin et al. (1978)
As	Solid solution		
Zn	Solid solution		
Mn	Solid solution	No, positive effect	
Fe	Precipitate as iron phosphide FeP_2		
Ni	Precipitate as nickel phosphide Ni_2P		
Sb	Solid solution, but close to solubility limit	Yes	
Sn	Solid solution	Yes	
Pb	Precipitate as Pb-phase	Yes	Yes
Bi	Precipitate as Bi-phase	Yes	Yes
B	Precipitate as B-phase	No, positive effect	
Ag	Precipitate as Ag-phase		
Cd	Solid solution, but close to solubility limit		
Hg	Precipitate with copper, Cu_7Hg_6		
Se	Precipitate with copper, Cu_2Se	Yes	Yes
Te	Precipitate with copper, Cu_2Te	Yes	Yes
O	Precipitate as copper phosphates $Cu_3(PO_4)_2$, or $Cu_2P_2O_7$	Yes	
S	Precipiate with copper, Cu_2S	Yes	Yes
P	Solid solution, but close to solubility limit	Reported to some extent	

In the work by Laporte and Mortensen, the positive effect of manganese was attributed to a patent that states manganese makes copper less sensitive to crack formation due to the strong deoxidising properties of manganese (Kubosono et al. 1995). No other reference has been found that experimentally show the positive effect of manganese in copper.

The positive influence of boron was based on two reports. One work was by Kanno et al. (1987), which demonstrated the positive influence of boron on bronze Cu-8Sn materials. The effect of boron was seen for ppm levels of boron. It was noted that with boron added, the grain boundaries become more mobile and the material shows less grain boundary cracking. The second work was by Suzuki and Itoh (1984), who investigated the influence of sulphur for several different pure copper grades. One of these grades was copper with 290 atppm boron, which showed a significant improvement in ductility compared to oxygen-free copper. Due to the low concentrations of both manganese and boron in OFP copper, these elements are not expected to show any significant positive influence on the ductility.

3.5 Iron, nickel and oxygen in OFP copper

Most of the impurity elements included in this study do not show any influence of phosphorus on its phase equilibria. The only exceptions are the three elements iron, nickel and oxygen.

Oxygen is known to cause embrittlement of copper. This has been studied by Nieh and Nix (1981) on oxygen containing copper. The influence on ductility was attributed to the segregation of oxygen to the grain boundaries and thus promoting intergranular fracture. It is known from the Cu-O binary (Magnusson and Frisk 2013) that the solubility of oxygen in copper is practically zero, and oxygen will form oxides. It should be noted that the negative effect of oxygen should be minimised by using "oxygen-free" copper with low concentrations of oxygen. Nevertheless, copper is sensitive to low concentrations of impurities and oxygen could be one of these.

A previous thermodynamic evaluation of the Cu-H-O-S-P system (Magnusson and Frisk 2013) showed that copper phosphates were more stable than copper oxide (Cu_2O) or any other phosphorus oxide (P_4O_{10}). Few experimental observations of copper phosphates exist in the literature. For this reason, OFP copper was carefully oxidised at low oxidising potentials in a previous work (Magnusson et al. 2016), in order to highlight the presence of these phosphates. Only the most stable oxides are stable to the lowest oxidising potentials, and it was experimentally verified that copper phosphates existed where copper oxides did not. However, copper phosphates have still not been seen in any high-resolution characterisation of OFP copper (Thuvander 2015, Andersson-Östling et al. 2017).

Iron has a low solubility in pure copper and forms metallic iron in phosphorus free copper. Iron in copper has not been reported to lower the ductility of coppers. The opposite material, with a minor copper content in an iron matrix is well known to precipitate nm-small copper particles at low temperatures. This is the basis for the precipitation hardened stainless steels which are often alloyed with a few wt% of copper. Phosphorus in OFP copper is expected to react with iron forming iron phosphides. Several possible iron phosphides exists which have a similar stability. Calculation with 10 wtppm iron and 50 wtppm phosphorus yields phosphide from 470 °C. The strong reaction between iron and phosphorus in copper has been verified in the literature, and actually led to the development of precipitation hardened high conductivity copper alloys. By keeping the iron to phosphorus atomic relation close to the Fe_2P stoichiometry, it is possible to produce a precipitation hardened alloy with high conductivity (Lu et al. 2006). These materials show tiny iron phosphides of 3–10 nm in size.

Nickel show high solubility in copper, but is expected to react with phosphorus in OFP copper. The nickel phosphides have lower stability compared to the corresponding iron variants. Calculations with 10 wtppm nickel and 50 wtppm phosphorus give nickel phosphides from 170 °C. Many of the nickel and iron phosphides share the same crystalline structure, and these elements can substitute in the phosphide. This has been shown experimentally by Nowotny and Henglein (1948). For this reason a combined precipitation of nickel plus iron could happen, but due to the lower stability of the nickel phosphide the nickel content will be limited.

4 Conclusions

Thermodynamic calculations have been made at room temperature for Cu-P-X alloying systems, where X stands for Pb, Zn, Fe, Ag, As, Sb, Te, Bi, Cd, Mn, Ni, Se, Sn, Hg, and B. The concentrations of impurities in OFP copper are assumed to be the maximum content according to material standards. Equilibrium calculations are made at room-temperature. The results for impurities and phosphorus in OFP copper are:

- Impurity occurring in solid solution: As, Zn, Mn, Sb, Sn, Cd, and P.
- Impurity precipitate occurring as inclusion, not containing copper: Pb, Bi, B, and Ag.
- Impurity precipitate occurring as inclusion with copper: Hg, Se, Te, and S.
- Impurity precipitate occurring as phosphorus compound: O (phosphate), Fe, and Ni (phosphides).

These results have been compared with reports on copper embrittlement. Classic embrittling elements in copper are bismuth, tellurium, lead, selenium and sulphur. All these elements will precipitate in copper due to a low solubility. It is noted that these reactions are not influenced by phosphorus.

Of all studied elements, the only elements that do show an influence of phosphorus are oxygen, nickel and iron. The phosphorus-oxygen interactions have been evaluated in a previous work, which indicated that copper phosphates are more stable than copper oxides. Both iron and nickel are expected to react with phosphorus forming phosphides. These two elements form phosphides with similar crystalline structure and can substitute. The iron phosphide has higher stability than the nickel variant, and is expected to be the most important one.

5 References

SKB's (Svensk Kärnbränslehantering AB) publications can be found at www.skb.se/publications.

An Mey S, 1992. Thermodynamic re-assessment of the Cu–Ni system. CALPHAD 16, 255–260.

Andersson-Östling H C M, Sandström R, 2009. Survey of creep properties of copper intended for nuclear waste disposal. SKB TR-09-32, Svensk Kärnbränslehantering AB.

Andersson-Östling H C M, Hagström J, Danielsson M, 2017. Phosphorous in copper intended for nuclear waste disposal. SKB R-17-19, Svensk Kärnbränslehantering AB.

Ansara I, Chatillon C, Lukas H L, Nishizawa T, Ohtani H, Ishida K, Hillert M, Sundman B, Argent B B, Watson A, Chart T G, Anderson T, 1994. A binary database for III–V compound semiconductor systems. CALPHAD 18, 177–222.

Arita M, Kamo K, 1985. Measurement of vapor pressure of phosphorus over Sn–P alloys by dew point method. Transactions of the Japan Institute of Metals 26, 242–250.

Barrera E V, Menyhard M, Bika D, Rothman B, McMahon C J, 1992. Quasi-static intergranular cracking in a Cu–Sn alloy; an analog of stress relief cracking of steels. Scripta Metallurgica et Mataerialia 27, 205–210.

Barin I, 1995. Thermochemical data of pure substances. 3rd ed. New York: VCH Publishers.

Berak J, Heumann T, 1950. Über das system mangan–phosphor. Zeitschrift für Metallkunde 41, 19–23. (In German.)

Carmalt C J, Cowley A H, Hector A L, Norman N C, Parkin I P, 1994. A synthesis of bismuth (III) phosphide: the first binary phosphide of bismuth. Journal of the Chemical Society, Chemical Communications 17, 1987–1988.

Chakrabarti D J, Laughlin D E, 1981. The Cu–Se (Copper–Selenium) system. Bulletin of Alloy Phase Diagrams 2, 305–315.

Chakrabarti D J, Laughlin D E, 1982. The B–Cu (Boron–Copper) system. Bulletin of Alloy Phase Diagrams 3, 45–48.

Chakrabarti D J, Laughlin D E, 1984a. The Bi–Cu (Bismuth–Copper) system. Bulletin of Alloy Phase Diagrams 5, 148–155.

Chakrabarti D J, Laughlin D E, 1984b. The Cu–Pb (Copper–Lead) system. Bulletin of Alloy Phase Diagrams 5, 503–510.

Chakrabarti D J, Laughlin D E, 1985. The Cu–Hg (copper–mercuy) system. Bulletin of Alloy Phase Diagrams 6, 522–527.

Chang L-S, Straumal B B, Rabkin E, Gust W, Sommer F, 1997. The solidus line of the Cu–Bi phase diagram. Journal of Phase Equilibria 18, 128–135.

Chang Y A, Goldberg D, Neumann J P, 1977. Phase diagrams and thermodynamic properties of ternary copper–silver systems. Journal of Physical and Chemical Reference Data 6, 645–646.

Chen Q, Jin Z, 1995. The Fe–Cu system, a thermodynamic evaluation. Metallurgical and Materials Transactions A 26A, 417–426.

Chen X-M, Liu L-B, Zhang L-G, Bo H, Jin Z-P, 2010. Thermodynamic assessment of Cu–Cd system. Transactions of Nonferrous Metals Society of China 20, 649–654.

David N, Fiorani J M, Vilasi M, Hertz J, 2003. Thermodynamic reevaluation of the Cu–Zn system by electromotive force measurements in the zinc-rich part. Journal of Phase Equilibria 24, 240–248.

Du Z, Guo C, Tao M, Li C, 2008. Thermodynamic modeling of the Cu–Se system. International Journal of Materials Research 99, 294–300.

Fujiwara S, Abiko K, 1995. Ductility of ultra high purity copper. Journal de Physique IV 5, 295–300.

Fürtauer S, Li D, Cupid D, Flandorfer H, 2013. The Cu–Sn phase diagram, Part I: New experimental results. Intermetallics 34, 142–147.

Gavin S A, Billingham J, Chubb J P, Hancock P, 1978. Effect of trace impurities on hot ductility of as-cast cupronickel alloys. Metals Technology 5, 397–401.

Gierlotka W, Chen S W, 2008. Thermodynamic descriptions of the Cu–Zn system, Journal of Materials Research 23, 258–263.

Gokcen N A, 1993. The Cu–Mn (copper–manganese) system. Journal of Phase Equilibria 14, 76–83.

Gullman J, Olofsson O, 1972. The crystal structure of SnP_3 and a note on the crystal structure of GeP_3. Journal of Solid State Chemistry 5, 441–445.

Gumiński C, 2005. The Hg–P (Mercury–Phosphorus) system. Journal of Phase Equilibria and Diffusion 26, 75.

Hansen M, Anderko K, 1958. Constitution of binary alloys. 2nd ed. New York: McGraw-Hill.

Hayes F H, Lukas H L, Effenberg G, Petzow G, 1986. A thermodynamic optimization of the Cu–Ag–Pd system. Zeitschrift für Metallkunde 77, 749–754.

He C, Du Y, Chen H-L, Liu S, Xu, H, Ouyang Y, Liu Z-K, 2008. Thermodynamic modeling of the Cu–Mn system supported by key experiments. Journal of Alloys and Compounds 457, 233–238.

Hino M, Ikubo S, Ohtani H, 2011. Thermodynamic analysis of the Cu–Sn–P ternary system. High Temperature Materials and Processes 30, 387–404.

Kanno M, Shimodaira N, Ohsako T, Suzuki H, 1987. Effects of a small amount of added elements on the ductility of a Cu–8 mass%Sn alloy at elevated temperatures. Transactions of the Japan institute of Metals 28, 73–80.

Karakaya I, Thompson W T, 1988. The Ag–P (Silver–Phosphorus) system. Bulletin of Alloy Phase Diagrams 9, 232–236.

Karakaya L, Thompson W, 1991. The As–P (arsenic–phosphorus) system. Journal of Phase Equilibria 12, 343–346.

Kaufman L, Nell J, Taylor K, Hayes F, 1981. Calculation of ternary systems containing III–V and II–VI compound phases. CALPHAD 5, 185–215.

Kowalski M, Spencer P J, 1993. Thermodynamic reevaluation of the Cu–Zn system. Journal of Phase Equilibria 14, 432–438.

Kubosono K, Asamizu I, Iwase M, Kurita T, 1995. Copper–nickel based alloy.
US patent 5441696.

Laporte V, Mortensen A, 2009. Intermediate temperature embrittlement of copper alloys. International Materials Reviews 54, 94–116.

Lee K J, Nash P, 1991. Ni–P (Nickel–Phosphorus) system. In Nash P (ed). Phase diagrams of binary nickel alloys. Materials Park, OH: ASM International, 235–246.

Li D, Franke P, Fürtauer S, Cupid D, Flandorfer H, 2013. The Cu–Sn phase diagram part II: New thermodynamic assessment. Intermetallics 34, 148–158.

Liang H, Chang Y A, 1998. A thermodynamic description for the Al–Cu–Zn system. Journal of Phase Equlibria 19, 25–37.

Liang S-M, Hsiao H-M, Schmid-Fetzer R, 2015. Thermodynamic assessment of the Al–Cu–Zn system, part I: Cu–Zn binary system. CALPHAD 51, 224–232.

Liu X J, Wang C P, Ohnuma I, Kainuma R, Ishida K, 2000. Thermodynamic assessment of the phase diagrams of Cu–Sb and Sb–Zn systems. Journal of Phase Equilibria 21, 432–442.

Liu Y, Wang G, Wang J, Chen Y, Long Z, 2012. Phase equilibria and thermodynamic functions for Ag–Hg and Cu–Hg binary systems. Thermochimica Acta 547, 83–88.

Lu D-P, Wang J, Zeng W-J, Liu Y, Lu L, Sun B-D, 2006. Study on high-strength and high-conductivity Cu–Fe–P alloys. Material Science and Engineering 421A, 254–259.

Lukas H L, Fries S G, Sundman B, 2007. Computational thermodynamics: the Calphad method. Cambridge: Cambridge University Press.

Magnusson H, Frisk K, 2013. Thermodynamic evaluation of Cu–H–O–S–P system. Phase stabilities and solubilities for OFP-copper. SKB TR-13-11, Svensk Kärnbränslehantering AB.

Magnusson H, Lindberg F, Frisk K, 2016. Validating thermodynamic description of copper oxides and phosphates by controlled oxidation of OFP-copper. SKB R-15-06, Svensk Kärnbränslehantering AB.

Miettinen J, 2001. Thermodynamic description of Cu–Sn–P system in the copper-rich corner. CALPHAD 25, 67–78.

Miettinen J, 2003. Thermodynamic description of the Cu–Al–Mn system in the copper-rich corner. CALPHAD 27, 103–114.

Miettinen J, Vassilev G, 2014a. Thermodynamic description of ternary Fe–X–P systems. Part 1: Fe–Cr–P. Journal of Phase Equilibria and Diffusion 35, 458–468.

Miettinen J, Vassilev G, 2014b. Thermodynamic description of ternary Fe–X–P systems. Part 2: Fe–Cu–P. Journal of Phase Equilibria and Diffusion 35, 469–475.

Miettinen J, Vassilev G, 2014c. Thermodynamic description of ternary Fe–X–P systems. Part 3: Fe–Mn–P. Journal of Phase Equilibria and Diffusion 35, 587–594.

Miettinen J, Vassilev G, 2015. Thermodynamic description of ternary Fe–X–P systems. Part 6: Fe–Ni–P. Journal of Phase Equilibria and Diffusion 36, 78–87.

Miodownik A P, 1994. Cu–Zn (Copper–Zinc). In Laughlin D E, Chakrabarti D J, Subramanian P R (eds). Phase diagrams of binary copper alloys. Materials Park, OH: ASM International, 487–496.

Moon K-W, Boettinger W J, Kattner U R, Biancaniello F S, Handwerker C A, 2000. Experimental and thermodynamic assessment of Sn–Ag–Cu solder alloys. Journal of Electronic Materials 29, 1122–1136.

Nieh T G, Nix D, 1981. Embrittlement of copper due to segregation of oxygen to grain boundaries. Metallurgical Transactions 12A, 893–901.

Niemelä J, Effenberg G, Hack K, Spencer R J, 1986. A thermodynamic evaluation of the copper–bismuth and copper–lead systems. CALPHAD 10, 77–89.

Nitsche R, May S A, Hack K, Spencer P, 1991. Thermodynamic evaluation of the copper–antimony system. Zeitschrift für Metallkunde 82, 67–72.

Noda T, Oikawa K, Itoh S, Hino M, Nagasaka T, 2009. Thermodynamic evaluation of Cu–Cu_3P system based on newly determined Gibbs energy of formation of Cu_3P. CALPHAD 33, 557–560.

Nowotny H, Henglein E, 1948. Ein beitrag zur Kenntnis ternärer Phosphorlegierungen. Monatshefte für Chemie und verwandte Teile anderer Wissenschaften 79, 385–393. (In German.)

Ohtani H, Hanaya N, Hasebe M, Teraoka S-I, Abe M, 2006. Thermodynamic analysis of the Fe–Ti–P ternary system by incorporating first-principles calculations into the Calphad approach. CALPHAD 30, 147–158.

Okamoto H, 1990a. Cd–P (Cadmium–Phosphorus). In Massalski T B, Okamoto H (eds). Binary alloy phase diagrams. Materials Park, OH: ASM International.

Okamoto H, 1990b. The Fe–P (iron–phosphorus) system. Bulletin of Alloy Phase Diagrams 11, 404–412.

Okamoto H, 1994. Cu–Te (Copper–Tellurium). In Subramanian P R (ed). Phase diagrams of binary copper alloys. Materials Park, OH: ASM International, 434–439.

Okamoto H, 2010. P–Te (Phosphorus–Tellurium). Journal of Phase Equilibria and Diffusion 31, 405–406.

Okamoto H, 2011. P–Zn (phosphorus–zinc) system. Journal of Phase Equilibria and Diffusion 32, 79.

Olofsson O, 1970. X-ray investigation of the Tin–Phosphorus system. Acta Chemica Scandinavica 24, 1153–1162.

Ozgowicz W, Biscondi M, 1995. High-temperature brittleness and interfacial segregation in tin bronzes. Journal de Physique IV 5, C7-315–320.

Pashinkin A S, Fedorov V A, 2003. Phase equilibria for the Cu–Te system. Inorganic Materials 39, 539–554.

Predel B, 1992. Phase equilibria, crystallographic and thermodynamic data of binary alloys. Volume 5B. Berlin: Springer.

Predel B, 1998. Phase equilibria, crystallographic and thermodynamic data of binary alloys. Volume 5I. Berlin: Springer.

Sandström R, Wu R, 2013. Influence of phosphorus on the creep ductility of copper. Journal of Nuclear Materials 441, 364–371.

Saunders N, Miodownik A P, 1998. Calphad: calculation of phase diagrams): a comprehensive guide. Oxford, UK: Elsevier.

Schlesinger M E, 2002. The thermodynamic properties of phosphorus and solid binary phosphides. Chemical Reviews 102, 4267–4301.

Schmetterer C, Vizdal J, Ipser H, 2009. A new investigation of the system Ni–P. Intermetallics 17, 826–834.

Shim J-H, Oh C-S, Lee B-J, Lee D N, 1996. Thermodynamic assessment of the Cu–Sn system. Zeitschrift für Metallkunde 87, 205–212.

SKB, 2010. Design, production and initial state of the canister. SKB TR-10-14, Svensk Kärnbränslehantering AB.

Spencer P J, 1986. A thermodynamic evaluation of the Cu–Zn system. CALPHAD 10, 175–185.

Subramanian P R, 1990. Cu–Sb (Copper–Antimony). In Massalski T B, Okamoto H (eds). Binary alloy phase diagrams. Materials Park, OH: ASM International.

Subramanian P R, Laughlin D. E, 1988. The As–Cu (Arsenic–Copper) system. Bulletin of Alloy Phase Diagrams 9, 605–618.

Subramanian P R, Laughlin D E, 1990. The Cd–Cu (Cadmium–Copper) system. Bullentin of Alloy Phase Diagrams 11, 160–169.

Subramanian P R, Perepezko J H, 1993. The Ag–Cu (silver–copper) system. Journal of Phase Equilibria 14, 62–75.

Suzuki H, Itoh G, 1984. A study of intermediate temperature embrittlement in pure copper. Journal of Japan Institute of Metals 48, 1016–1021.

Swartzendruber L J, 1993. Cu–Fe (Copper–Iron). In Okamoto H (ed). Phase diagrams of binary iron alloys. Materials Park, OH: ASM International, 131–137.

Teppo O, Taskinen P, 1991. Critical assessment of the thermodynamic properties of antimony–copper alloys. Scandinavian Journal of Metallurgy 20, 174–182.

Teppo O, Niemelä J, Taskinen P, 1990. An assessment of the thermodynamic properties and phase diagram of the system Bi–Cu. Thermochimica Acta 173, 137–150.

Teppo O, Niemelä J, Taskinen P, 1991. The copper–lead phase diagram. Thermochimica Acta 185, 155–169.

Thuvander M, 2015. Investigation of the distribution of phosphorus in copper. Report 2015:11, Strålsäkerhetsmyndigheten (Swedish Radiation Safety Authority).

Tu H, Yin F, Su X, Liu Y, Wang X, 2009. Experimental investigation and thermodynamic modeling of the Al–P–Zn ternary system. CALPHAD 33, 755–760.

Turchanin M A, Agraval P G, Nikolaenko I V, 2003. Thermodynamics of alloys and phase equilibria in the copper–iron system. Journal of Phase Equilibria 24, 307–319.

Turchanin M A, Agraval P G, Abdulov A R, 2007. Phase equilibria and thermodynamics of binary copper systems with 3d-metals. VI. Copper–nickel system. Powder Metallurgy and Metal Ceramics 46, 467–477.

Uhland S, Lechtman H, Kaufman L, 2001. Assessment of the As–Cu–Ni system: an example from archaeology. CALPHAD 25, 109–124.

Wagman D D, Evans W H, Parker V B, Schumm R H, Halow I, Bailey S M, Chruney K L, Nuttall R L, 1982. The NBS tables of chemical thermodynamic properties. Journal of Physical and Chemical Reference Data 11, supplement No. 2.

Wang C P, Li X J, Ohnuma I Kainuma R Ishida K, 2000. Thermodynamic assessment of the Cu–Ni–Pb system. CALPHAD 24, 149–167.

Wang C P, Guo S H, Tang A T, Pan F S, Liu X J, Ishida K, 2009. Thermodynamic assessments of the Cu–B and Cu–Tm systems. Journal of Alloys and Compounds 482, 67–72.

Wang J, Liu C, Leinenbach C, Klotz U E, Uggowtzer P J, Löffler J F, 2011. Experimental investigation and thermodynamic assessment of the Cu–Sn–Ti ternary system. CALPHAD 35, 82–94.

Wang J, Xu H, Shang S, Zhang L, Du Y, Zhang W, Liu S, Wang P, Liu Z-K, 2011. Experimental investigation and thermodynamic modeling of the Cu–Si–Zn system with the refined description for the Cu–Zn system. CALPHAD 35, 191–203.

Zaikina J V, Kovnir K A, Sobolev A N, Presniakov I A, Kytin V G, Kulbachinskii V A, Olenev A V, Lebedev O I, Van Tendeloo G, Dikarev E V, Shevelkov A V, 2008. Highly disordered crystal structure and thermoelectric properties of Sn_3P_4. Chemistry of Materials 20, 2476–2483.

Zhang W-W, Du Y, Xy H, Xiong Y, Sun W, Pan F, Tang A, 2009. Thermodynamic assessment of the Cu–B system supported by key experiments and first-principles calculations. Journal of Phase Equilibria and Diffusion 30, 480–486.

Appendix A

Review of alloying systems and calculations

A1 Cu-X systems

A1.1 Cu-As

The Cu-As system has been reviewed by Subramanian and Laughlin (1988). The Cu-As system has been thermodynamically evaluated by Uhland et al. (2001). The calculated Cu-As phase diagram according to their presented parameters is calculated and shown in Figure A-1. Some disagreement is seen for the liquid, but is accurate up to a few percent of arsenic. The alpha-phase contains up to 7 at% of arsenic before arsenic precipitates as beta-phase Cu_7As. The most dominant intermediate phase is the gamma-phase Cu_3As, which is stable from liquid down to room temperature.

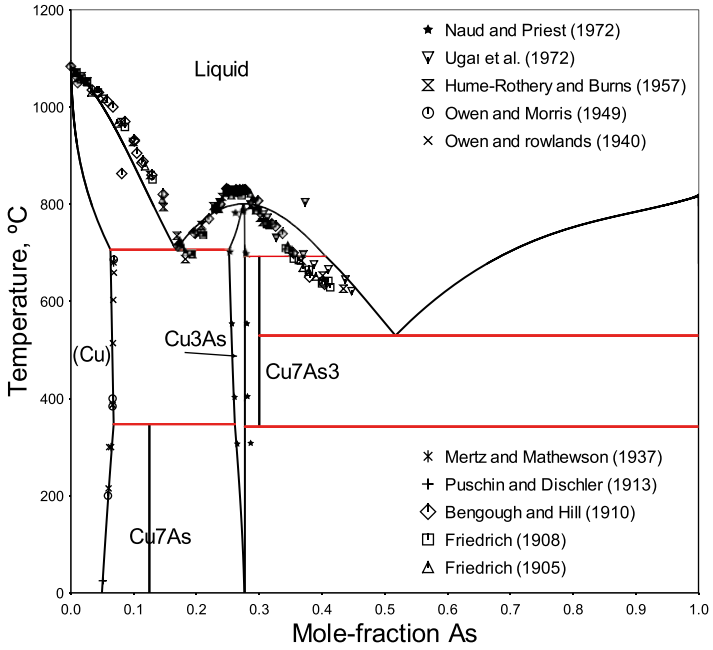

Designation, and typical composition[1, 2]		Space group[1]
α	Cu	$Fm\bar{3}m$
β	Cu_9As, Cu_7As[2]	$P6_3/mmc$
γ (HT)	Cu_3As	$P6_3/mmc$
γ' (LT)	Cu_3As	$P\bar{3}c1$
δ (HT)	Cu_5As_2, Cu_7As_3[2]	$Fm\bar{3}m$
δ' (LT)	Cu_5As_2, Cu_7As_3[2]	$Ibam$
As	As	$R\bar{3}m$

[1] Data taken from Subramanian and Laughlin (1988).

[2] Specific data taken from Uhland et al. (2001).

Figure A-1. *Cu-As binary phase diagram according to evaluation by Uhland et al. (2001). Experimental data is according to review by Subramanian and Laughlin (1988).*

A1.2 Cu-Zn

The Cu-Zn binary system is well-studied since it covers brass alloys. It has been studied many times in the past. The first detailed evaluation was made by Spencer (1986). Other evaluations are Kowalski and Spencer (1993), Liang and Chang (1998), David et al. (2003), Gierlotka and Chen (2008), and Wang et al. (2011). The most recent evaluation is given by Liang et al. (2015), which also summaries previous work. The Cu-Zn phase diagram calculated using the parameters by Liang et al. is presented in Figure A-2. Since this system is well studied no experimental data is given in detail here. More than 100 experimental references were used in the experimental review by Miodownik (1994), and the experimentally determined solubility limit of zinc in metallic copper is shown in Figure A-2 as reference.

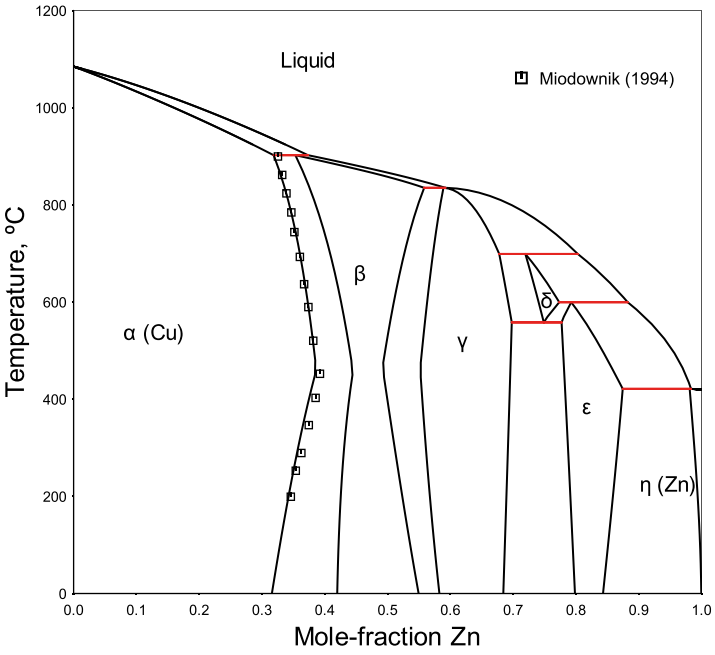

Designation, and typical composition[1]		Space group[1]
α	Cu	$Fm\bar{3}m$
β (HT)	45 at% Zn	$Im\bar{3}m$
β' (LT)	45 at% Zn	$Pm\bar{3}m$
γ	60 at% Zn	$I\bar{4}3m$
δ	77 at% Zn	$C_{3h}{}^1P\bar{6}$
ε	80 at% Zn	$P6_3/mmc$
η	Zn	$P6_3/mmc$

[1] Data taken from Liang et al. (2015).

Figure A-2. *Calculated Cu-Zn binary using the parameters from Liang et al. (2015). Experimentally determined phase boundary from review by Miodownik (1994).*

A1.3 Cu-Mn

The Cu-Mn system has been evaluated many times in the past. Two of the more recent ones are the evaluations by Miettinen (2003) and He et al. (2008). The differences between these evaluations are minor, and the older one by Miettinen will be used in this work due to their evaluations of the ternary P-Mn system. The calculated phase diagram for the Cu-Mn system is shown in Figure A-3. The experimental data regarding the Cu-Mn system has been summarised by Gokcen (1993). The manganese γ-phase shares the same crystalline structure as copper and forms a solid solution phase with copper. Copper is expected to have a high solubility of manganese.

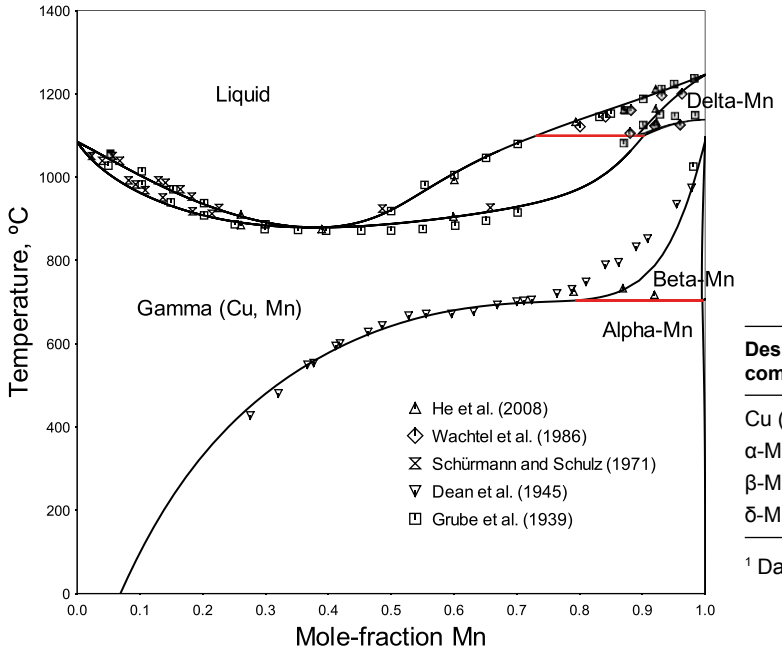

Designation, and typical composition[1]		Space group[1]
Cu (γ-Mn)	0–100 wt% Mn	$Fm\bar{3}m$
α-Mn	99.7–100 wt% Mn	*cI*58
β-Mn	99.5–100 wt% Mn	*cP*20
δ-Mn	85.8–100 wt% Mn	$Pm\bar{3}m$

[1] Data taken from Gokcen (1993).

Figure A-3. *Calculated Cu-Mn binary system using the parameters from Miettinen (2003). Experimental data is taken from the thermodynamic evaluation by He et al. (2008).*

A1.4 Cu-Fe

The Cu-Fe system has been thermodynamically assessed many times. The most used evaluation is the one by Chen and Jin (1995). This evaluation was also used by Miettinen and Vassilev (2014b) in their evaluation of the ternary Cu-Fe-P system. Another more recent evaluation is Turchanin et al. (2003). The differences in their evaluations are minor, especially when considering the copper-rich part of the system. Since the evaluation by Chen and Jin was used in the ternary evaluation of the Cu-Fe-P system, the work by Chen and Jin will be followed in this work. The Cu-Fe binary system has been calculated and is presented in Figure A-4. The solubility of iron in metallic copper is low, verified by some experiments from the literature. The solubility falls with temperature and the extrapolated solubility indicates that the solubility is less than a wtppm at room temperature. Iron will not be in solid solution in OFP copper, and will be found in some inclusion. The Cu-Fe system is of commercial interest in precipitation hardened stainless steel, where copper particles are known to precipitate as nm-small metallic phases in iron matrix.

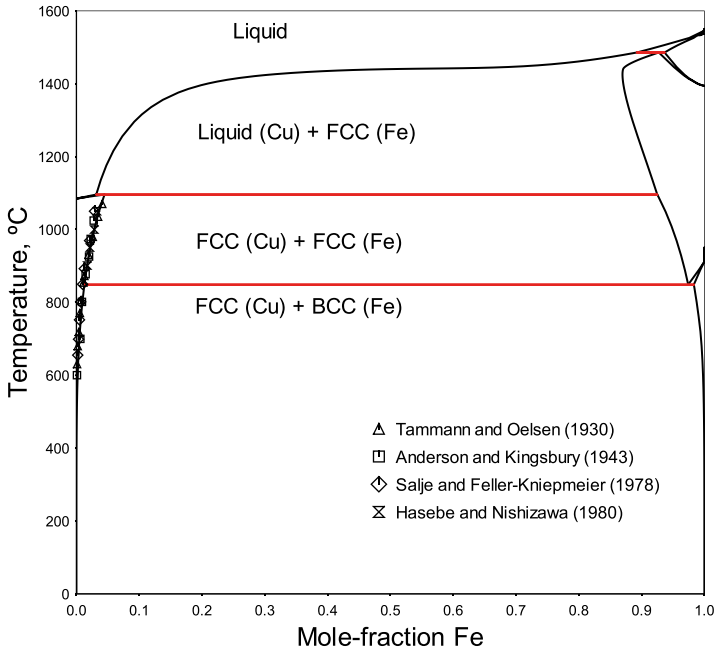

Designation, and typical composition[1]		Space group[1]
Cu (FCC)	0–5 wt% Fe	$Fm\bar{3}m$
α-Fe (BCC)	98–100 wt% Fe	$Im\bar{3}m$
γ-Fe (FCC)	85–100 wt% Fe	$Fm\bar{3}m$
δ-Fe (BCC, HT)	92–100 wt% Fe	$Im\bar{3}m$

[1] Data taken from Swartzendruber (1993).

Figure A-4. *Cu-rich part of the Fe-Cu binary system. Parameters and experimental data according to the evaluation by Chen and Jin (1995).*

A1.5 Cu-Ni

The Cu-Ni system is a simple system consisting of the liquid phase and the FCC type of phase. The main difficulty is the miscibility gap in the FCC structure at low temperature. This gives Cu-rich and Ni-rich FCC phases. The system has been assessed thermodynamically several times in the past. The most used description is the work by An Mey (1992), but it has also been more recently evaluated by Turchanin et al. (2007). The differences between these two evaluations are minor. The calculated Cu-Ni diagram is presented in Figure A-5, based on the thermodynamic evaluation by An Mey (1992). The solubility of nickel in the Cu-rich FCC phase at room temperature is 3.9 wt%. Due to slow element diffusion at low-temperatures, it is difficult to exactly determine the phase boundaries of the miscibility gap.

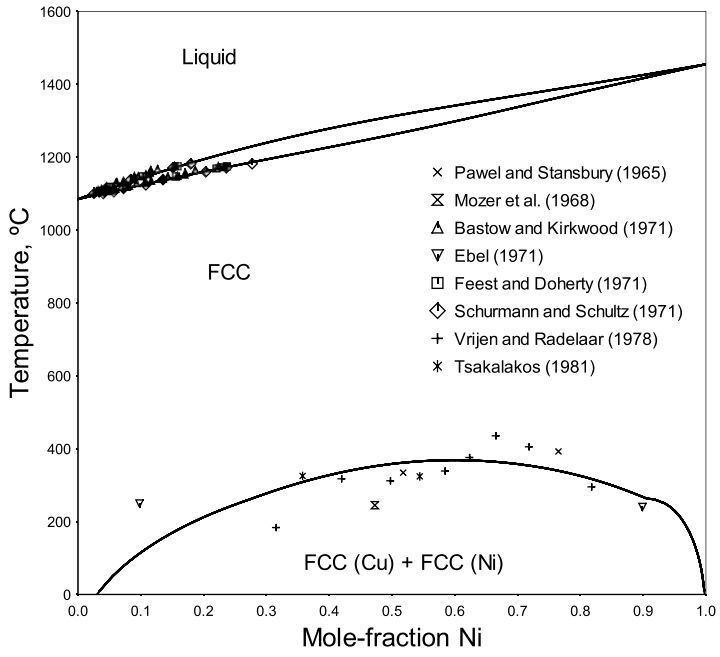

Designation, and typical composition		Space group
Cu,Ni (FCC)	0–100 wt% Ni	$Fm\bar{3}m$

Figure A-5. *Calculated Cu-Ni system using the parameters from the evaluation by An Mey (1992). References to experimental data can be found in the evaluation by Turchanin et al. (2007).*

A1.6 Cu-Sb

Liu et al. (2000) have made the most recent evaluation of the Cu-Sb system. Some older evaluations exist as well, such as the works by Nitsche et al. (1991) and Teppo and Taskinen (1991). The main improvement in the work by Liu et al. is that the Cu-Sb β-phase should be treated as an ordered BCC (A2) structure, rather than the disordered FCC structure used in the older evaluations. This is mainly of importance for calculations for higher-ordered systems where this phase appears. The solubility of antimony in copper is low at room-temperature. The calculated solubility is 11 wtppm.

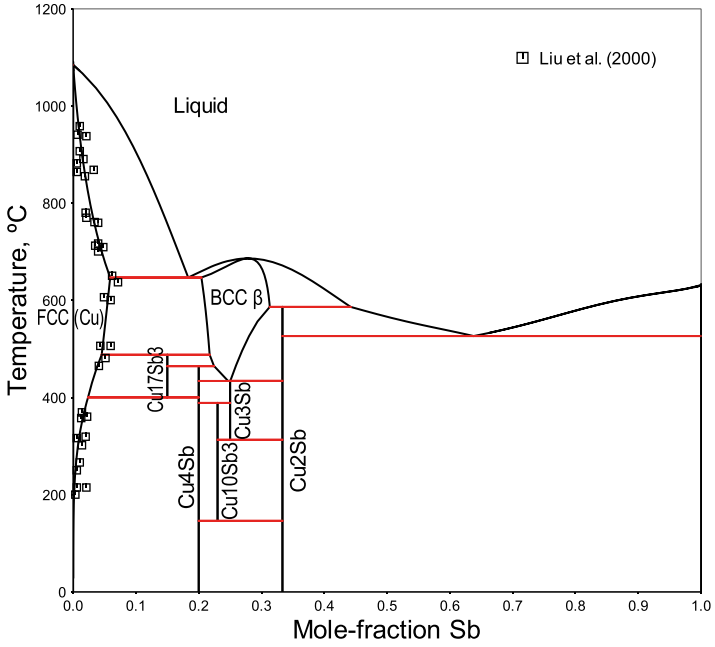

Designation, and typical composition[1, 2]		Space group[1]
α-Cu (FCC)	0–10.6 wt% Sb	$Fm\bar{3}m$
β (BCC)	31.6–46 wt% Sb	$Fm\bar{3}m$
γ $Cu_{17}Sb_3$	26–26.7 wt% Sb	$P6_3/mmc$
δ Cu_4Sb	30.3–32 wt% Sb	$P6_3/mmc$
ε Cu_3Sb	36.1–39.4 wt% Sb	$Pmmn$
ζ $Cu_{10}Sb_3$	34.1–34.5 wt% Sb	$P\bar{3}$
η Cu_2Sb	47.4–48.9 wt% Sb	$P4/nmm$
Cu,Ni (FCC)	100 wt% Sb	$R\bar{3}m$

[1] Data taken from Subramanian (1990).
[2] Designation follows Liu et al. (2000).

Figure A-6. *Calculated Cu-Sb system using the parameters from the evaluation by Liu et al. (2000). Experimental summarised by Liu et al.*

A1.7 Cu-Sn

Cu-Sn alloys constitute tin bronzes, which have been of interest since the Bronze Age. The alloying system has also received renewed interest due to the aim of developing lead-free solders for the microelectronic industry. The Cu-Sn system has been evaluated many times in the past. Three more recent evaluations are the works by Shim et al. (1996), Wang et al. (2011), and by Li et al. (2013). Wang et al. continued on the older work by Shim et al. which was later also used by Miettinen (2001) in his evaluation of the ternary Cu-P-Sn system. Li et al. made improvements in the thermodynamic description of Cu-Sn of intermediate phases β and γ bronzes by modelling these phases with order/disorder models. However, for the copper rich α-phase and the solubility of tin in metallic copper, minor differences are seen between these three evaluations. The parameters by Wang et al. will be used in this work. The calculated solubility of tin in copper at room temperature is 1.5 wt%.

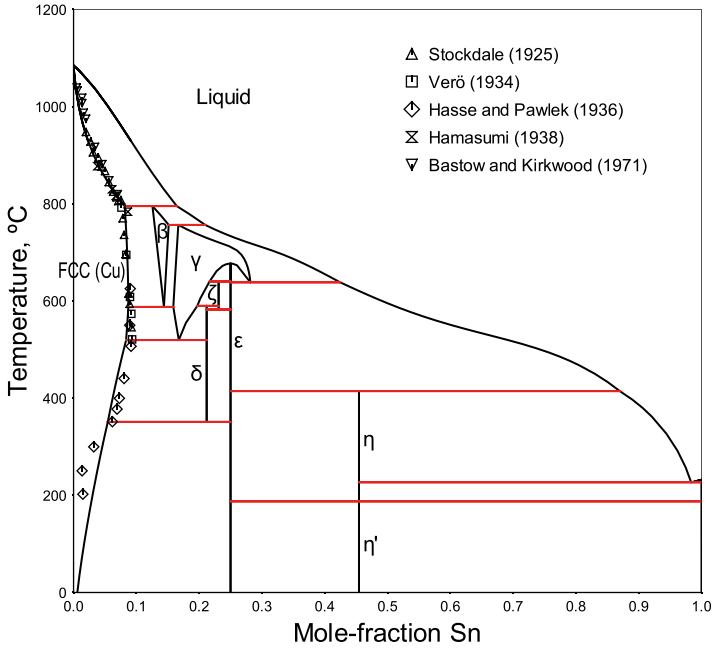

Designation, and typical composition[1]		Space group[1]
Cu	0–16 wt% Sn	$Fm\bar{3}m$
β	$Cu_{17}Sn_3$	$Im\bar{3}m$
γ	Cu_3Sn	$Fm\bar{3}m$
B2-bcc	No data	$Pm\bar{3}m$
δ	$Cu_{41}Sn_{11}$	$F\bar{4}3m$
ε	Cu_3Sn	*Cmcm*
ζ	$Cu_{10}Sn_3$	$P6_3$
η	Cu_6Sn_5	$P6_3/mmc$
η'	Cu_6Sn_5	*C2/c*
Sn	100 wt% Sn	*I41/amd*

[1] Data taken from Fürtauer et al. (2013).

Figure A-7. *Calculated Cu-Sn binary system using the parameters by Wang et al. (2011). Experimental data, with references, are taken from Li et al. (2013).*

A1.8 Cu-Pb

The Cu-Pb system has been of traditional interest for brass alloys, where lead is added to improve the machinability of the material. Lead shows little interaction with other metallic elements and solidifies at low temperature as a separate inclusion. Several different thermodynamic assessments of the alloying system Cu-Pb exists. Some of the more important ones are Teppo et al. (1991), and by Wang et al. (2000). In this work the parameters by Teppo et al. will be used. By using the parameters by Wang et al. it was not possible to reproduce the calculated Cu-Pb binary. The calculated phase diagram is presented in Figure A-8. The calculation is compared with experimental observations, which has been summarised by Teppo et al. by taking data from thirteen different references. Max solubility of lead in metallic copper is 1.3wt% at around 950 °C. The solubility then falls with temperature and is lower than 1 wtppm at room temperature.

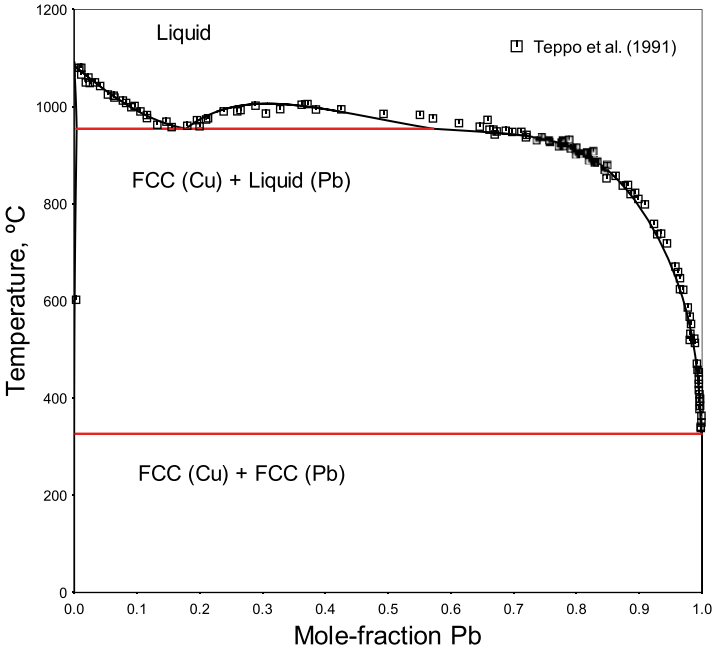

Designation, and typical composition[1]		Space group[1]
Cu	0–1 wt% Pb	$Fm\bar{3}m$
Pb	~100 wt% Pb	$Fm\bar{3}m$

[1] Data taken from Chakrabarti and Laughlin (1984b).

Figure A-8. *Calculated Cu-Pb binary system using the parameters by Teppo et al. (1991). Experimental data summarised for thirteen different references by Teppo et al.*

A1.9 Cu-Bi

The Cu-Bi system share many similarities with the Cu-Pb system. Bismuth is, like lead, a low-melting specie with little solubility in metallic copper. No intermediate phases are present and the solubility of bismuth in copper is very low. This simple binary system has been studied several times. The most detailed work seems to be by Teppo et al. (1990). A previous work was made by Niemelä et al. (1986), but this work did not contain any information about bismuth solubility in copper. Chang et al. (1997) produced some additional experiments on bismuth solubility in metallic copper, and made also a thermodynamic evaluation but using other thermodynamic model for the liquid. The calculated Cu-Bi binary phase diagram is presented in Figure A-9 using the description by Teppo et al. The maximum solubility of bismuth in copper takes place close to 950 °C and is 0.03wt% bismuth. At room temperature the solubility of bismuth is much lower than one wtppm.

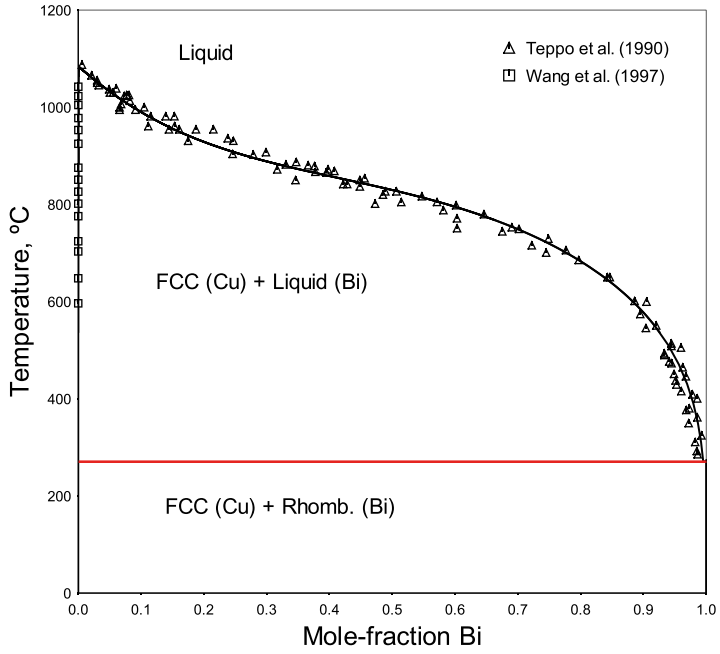

Designation, and typical composition[1]		Space group[1]
Cu	~0 wt% Bi	$Fm\bar{3}m$
Bi	~100 wt% Bi	$R\bar{3}m$

[1] Data taken from Chakrabarti and Laughlin (1984a).

Figure A-9. *Calculated Cu-Bi binary system using the parameters by Teppo et al. (1990). Experimental data for liquidus is summarised for ten different references by Teppo et al. Additional data for bismuth solubility in copper is Chang et al. (1997)*

A1.10 Cu-B

The Cu-B binary system is a simple eutectic system consisting of end-members copper and boron, and the liquid phase. An experimental review has been made by Chakrabarti and Laughlin (1982). Copper has a low solubility of boron, only 0.05 wt% has been reported as maximum, according to Chakrabarti and Laughlin. Only two thermodynamic evaluations have been found in the literature, which are the works by Wang et al. (2009) and Zhang et al. (2009). These evaluations have been made at the same time independently of each other. In this work the evaluation by Wang et al. is chosen, motivated by a better agreement to experiments including the liquid phase. The calculated Cu-B binary using the parameters by Wang et al. is presented in Figure A-10. The calculated maximum solubility of boron in copper at the eutectic point, close to 1000 °C, is 0.08wt%. The solubility then falls with temperature and at room temperature the extrapolated solubility is much lower than one wtppm.

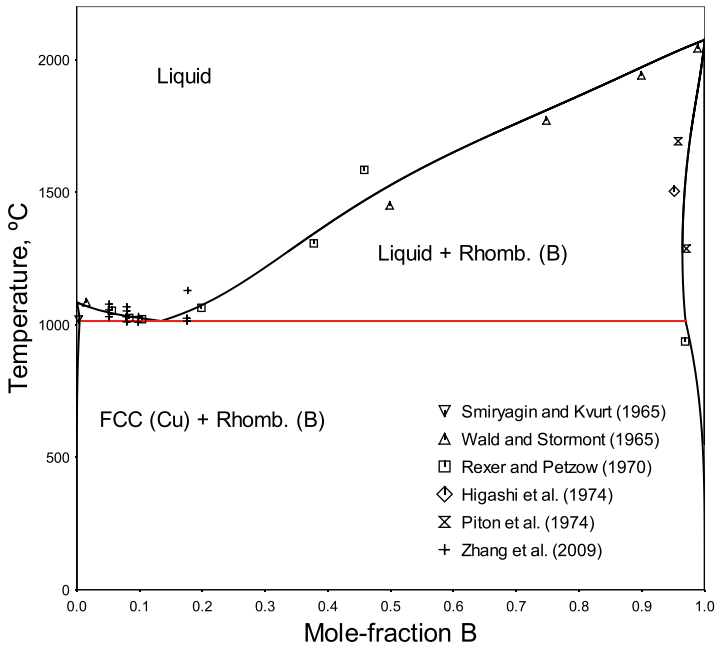

Designation, and typical composition[1]		Space group[1]
Cu	~0 wt% B	$Fm\bar{3}m$
β-B	85–100 wt% B	$R\bar{3}m$

[1] Data taken from Chakrabarti and Laughlin (1982).

Figure A-10. *Calculated Cu-B binary system using the parameters by Wang et al. (2009). Experimental data with references is taken from Wang et al. except the reference Siryaagin and Kvurt (1965) and Zhang et al. (2009), which are taken from Zhang et al. (2009).*

A1.11 Cu-Ag

The Cu-Ag system has been thermodynamically assessed by Hayes et al. (1986), and more recently by Moon et al. (2000). This binary system is of interest since it is one part of a thermodynamic database for lead-free solders. A review of the experimental data regarding the Cu-Ag system has been given by Subramanian and Perepezko (1993). The Cu-Ag binary system is calculated and presented in Figure A-11, using the parameters by Moon et al. The calculation is compared with experimental data taken from the review by Subramanian and Perepezko. The calculated solubility at room temperature is 0.5 wtppm.

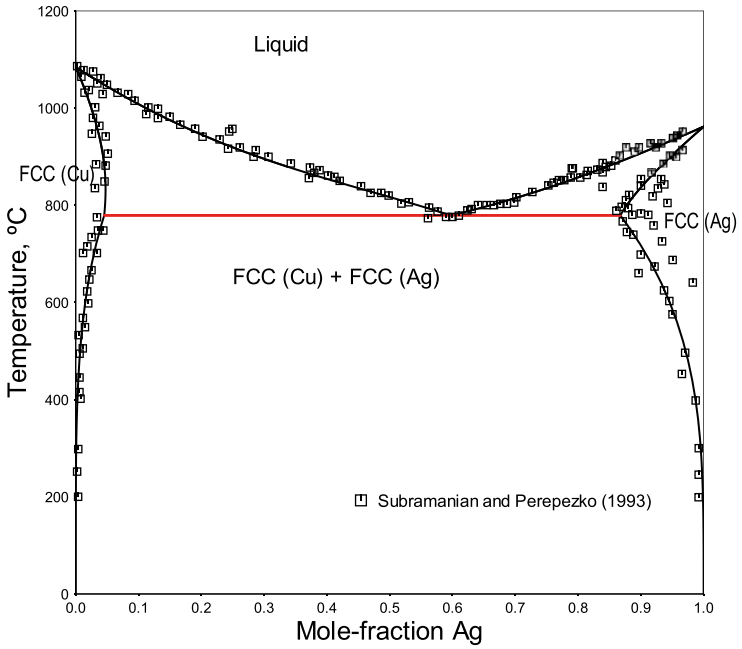

Designation, and typical composition[1]		Space group[1]
Cu	0–7.4 wt% Ag	$Fm\bar{3}m$
Ag	91.8–100 wt% Ag	$Fm\bar{3}m$

[1] Data taken from Subramanian and Perepezko (1993).

Figure A-11. *Calculated Cu-Ag binary system using the parameters by Moon et al. (2000). Experimental data is taken from the review by Subramanian and Perepezko (1993), who summarised data from 13 different references.*

A1.12 Cu-Cd

Only one thermodynamic assessment has been made on the Cu-Cd system, which is the work by Chen et al. (2010). They assessed the system based on the experimental data summarised in the review by Subramanian and Laughlin (1990). The calculated system is shown in Figure A-12, together with experimental data for cadmium solubility in metallic copper. The solubility at 550 °C is 3.8 wt% cadmium, and is extrapolated to 3 wtppm at room temperature.

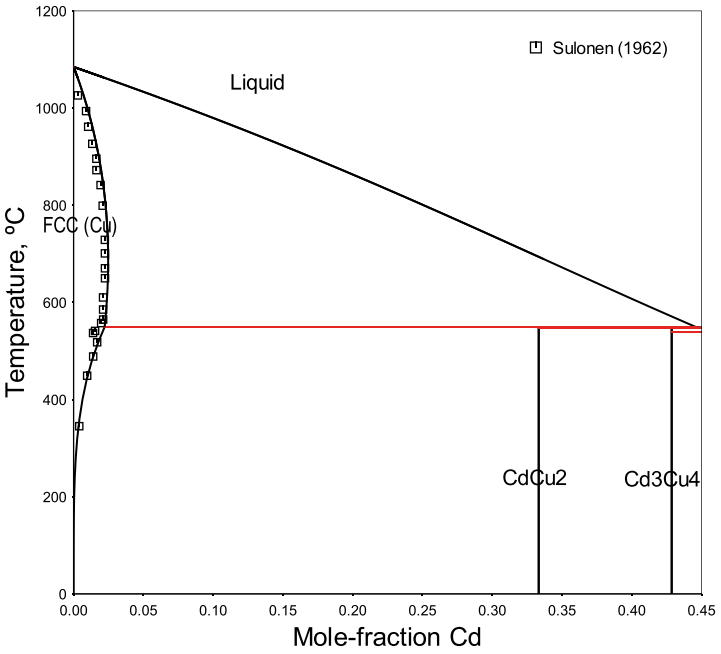

Designation, and typical composition[1, 2]		Space group[1]
Cu	0–3.6 wt% Cd	$Fm\bar{3}m$
β ($CdCu_2$)	46.9 wt% Cd	$P6_3/mmc$
γ (Cd_3Cu_4)	~57 wt% Cd	$F\bar{4}3m$
δ (Cd_5Cu_8)	66–77 wt% Cd	*?*
ε ($Cd_{10}Cu_3$)	~85 wt% Cd	$P6_3/mmc$
Cd	~100 wt% Cd	$P6_3/mmc$

[1] Data taken from Subramanian and Laughlin (1990).

[2] Phase designations follows the work by Chen et al. (2010).

Figure A-12. *Calculated Cu-Cd binary system using the parameters by Chen et al. (2010). Experimental data with references is taken from the same work.*

A1.13 Cu-Hg

One thermodynamic evaluation for the Cu-Hg system has been found in the literature, the work by Liu et al. (2012). There seems to be some typing error in their reported parameters and it is difficult to reproduce the mercury-rich part of the system. On the other hand, the Cu-rich part up to 50 at% is well described as illustrated in Figure A-13. An experimental review of the system has been made by Chakrabarti and Laughlin (1985). The calculated solubility of mercury in copper at room temperature is much lower than 1 wtppm.

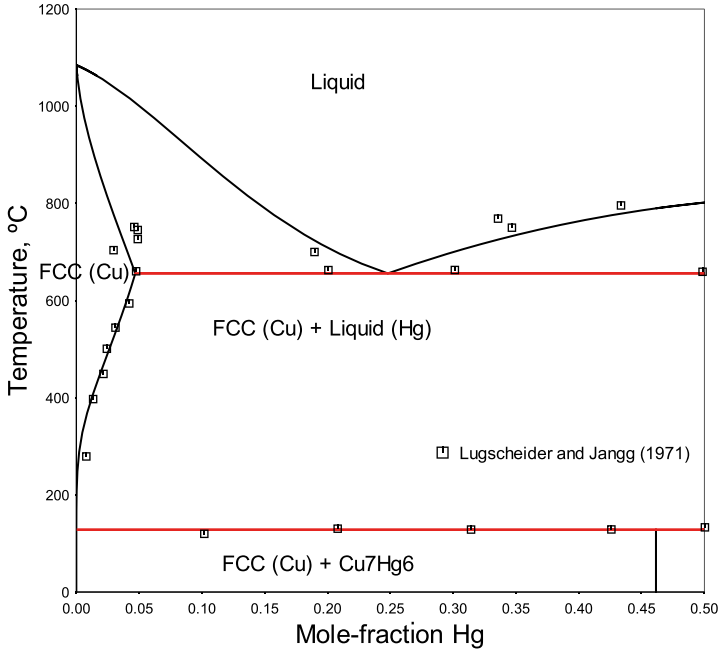

Designation, and typical composition[1, 2]		Space group[1]
Cu	0–15 wt% Hg	$Fm\bar{3}m$
γ (Cu_7Hg_6)	73 wt% Hg	$R\bar{3}m$
α Hg	~57 wt% Cd	$R\bar{3}m$
β Hg	66–77 wt% Cd	$I4/mmm$

[1] Data taken from Chakrabarti and Laughlin (1985).

[2] Phase designations follows the work by Liu et al. (2012).

Figure A-13. *Calculated Cu-Hg binary system using the parameters by Liu et al. (2012). Experimental data with references is taken from the same work.*

A1.14 Cu-Se

The experimental data belonging to the Cu-Se system has been evaluated by Chakrabarti and Laughlin (1981), and thermodynamically assessed by Du et al. (2008). Unfortunately, some of the reported parameters are not correct and it is not possible to reproduce the whole Cu-Se system. The most important selenide is Cu_2Se, which exists as α and β phases. The copper-rich part of the Cu-Se binary is shown in Figure A-14.The calculated solubility of selenium in copper is low already at high temperature, and is much lower than a one wtppm at room temperature. Du et al. makes no attempt to model the solid solution since it is practically zero.

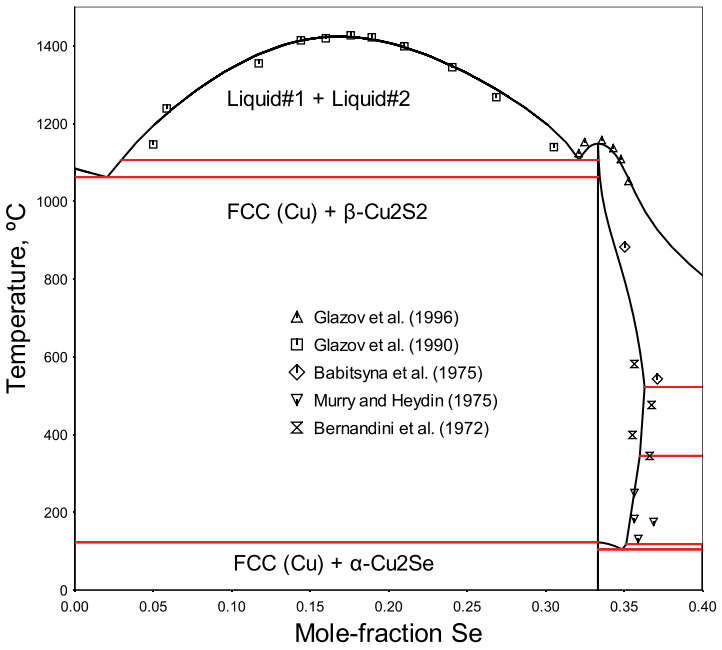

Designation, and typical composition[1]		Space group[1]
Cu	~0 wt% Se	$Fm\bar{3}m$
α-Cu_2Se	~38 wt% Se	
β-Cu_2Se	38–41 wt% Se	$Fm\bar{3}m$
Cu_3Se_2	45 wt% Se	$P\bar{4}2_1$ m
α-CuSe	73 wt% Hg	$P6_3/mmc$
β-CuSe	~57 wt% Cd	
γ-CuSe	66–77 wt% Cd	$P6_3/mmc$
$CuSe_2$	66–77 wt% Cd	$Pnnm$
Se	66–77 wt% Cd	$P3_1$ 21

[1] Data taken from Chakrabarti and Laughlin (1981).

Figure A-14. *Calculated Cu-Se binary system using the parameters by Du et al. (2008). Experimental data with references is taken from the same work.*

A1.15 Cu-Te

No thermodynamic assessment has been found for the Cu-Te system. An experimental review has been made by Pashinkin and Fedorov (2003), and their estimated phase diagram is presented in Figure A-15. The main complexity of the system is the many polymorphs of the Cu_2Te phase, labelled A-N. In similarity with the related systems Cu-Se and Cu-S, the solubility of tellurium in copper is practically zero. The solubility of Te in copper can be estimated from the solubility product $\log x = -7372/T + 2.43$ (Pashinkin and Fedorov 2003), where x is the mole-fraction of Te and T is absolute temperature. This expression indicates that the solubility is 1 atppm at 600 °C, and falling with temperature.

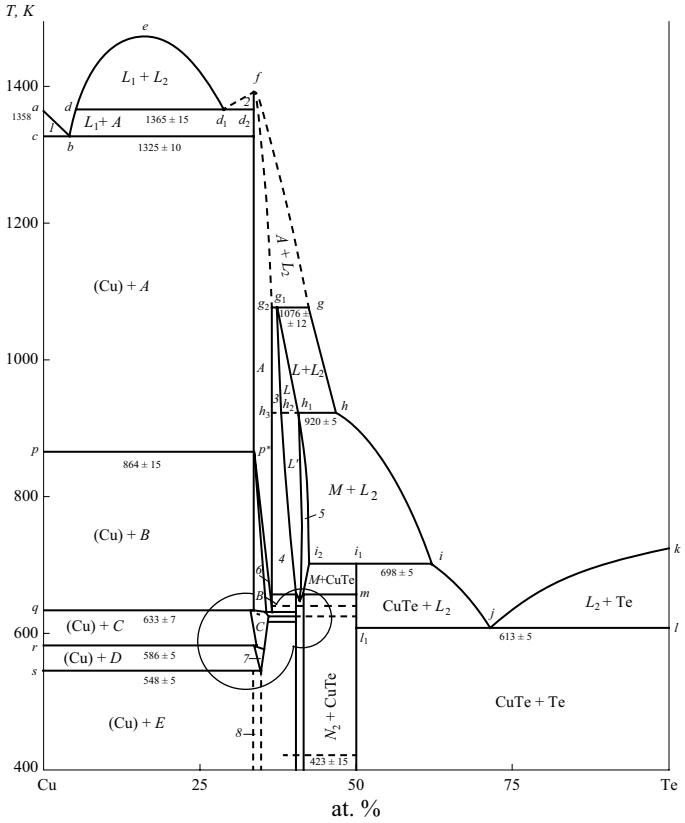

Designation, and typical composition[1]		Space group[1]
Cu	~0 wt% Te	$Fm\bar{3}m$
A (Cu2Te)	50–53.6 wt% Te	$Fd\bar{3}m$
B (Cu2Te)	50–53 wt% Te	*P6/mmm*
No space group reported for following (Cu_2Te) variants: C, D, E, F, G, I, J, L', M, N		
H (Cu2Te)	52–53 wt% Te	*P3m1*
K	52.9–53.3 wt% Te	*P3m1*
L	54–58 wt% Te	*P4/nmm*
CuTe	67 wt% Te	*Pmmn*
Te	100 wt% Te	$P3_1\,21$

[1] Data taken from Okamoto (1994), also available in Pashinkin and Fedorov (2003).

Figure A-15. *Cu-Te phase diagram according to experimental evaluation by Pashinkin and Fedorov (2003).*

A2 Cu-P-X systems

A2.1 Cu-P-As

The P-As system has been evaluated by Ansara et al. (1994), which originates from an older work by Kaufman et al. (1981). The system has limited experimental data, reviewed by Karakaya and Thompson (1991). Three solid solution phases exists, the end-members arsenic and phosphorus, plus AsP. There seems to be an error in the reported parameter for phosphorus solid solution in the arsenic rich end-member. In the paper by Ansara et al. a value of ${}^0G_{As,P}^{Rhomb} = 106\,922$ is stated, but should be ten times lower and ${}^0G_{As,P}^{Rhomb} = 10\,692.2$ is used in this work. The calculated phase diagram is shown in Figure A-16.

Combining the As-P binary by Ansara et al. with Cu-P binary (Noda et al. 2009), and Cu-As given in Section A1.1 (Uhland et al. 2001) makes it possible to calculate equilibria for the Cu-P-As system. Calculated equilibrium with 5 wtppm arsenic and 50 wtppm phosphorus at room temperature indicates that arsenic should remain in solid solution. Copper has a high solubility of arsenic, and the first forming phosphide when raising the phosphorus content is Cu_3P, at approximately 500 wtppm phosphorus (Magnusson and Frisk 2013).

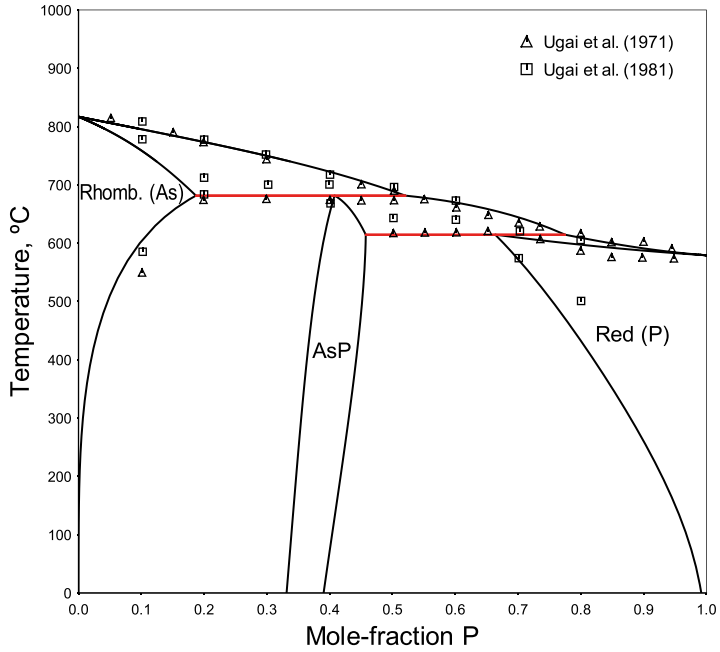

Designation, and typical composition[1]		Space group[1]
As	~0 wt% P	$R\bar{3}m$
AsP	~21.5 wt% P	
P (Red)	43–100 wt% P	

[1] Data taken from Karakaya and Thompson (1991).

Figure A-16. *Calculated As-P binary system using the parameters by Ansara et al. (1994). Experimental data with references is taken from the same work.*

A2.2 Cu-P-Zn

The P-Zn binary system has been assessed by Tu et al. (2009), and the calculated phase diagram is shown in Figure A-17. Okamoto (2011) has made a review of the experimental data to this system. However, when applying the parameters by Tu et al. it was found that their description could not be used since the calculated formation energies were much higher than reported in their work. For this reason, their thermodynamic parameters will not be used in this work. However, Tu et al. summarised the thermochemical data, and the reported Gibbs energy of formation for the phosphides will be used. The used Gibbs energies are Zn_3P_2 180.1 kJ/mole, and 122.9 kJ/mole for ZnP_2 (Tu et al. 2009).

Calculations for the Cu-P-Zn system is made based on data from the two binaries Cu-P (Noda et al. 2009) and Cu-Zn as presented in Section A1.2 (Liang et al. 2015) plus the reported Gibbs energies of formations for the two phosphides Zn_3P_2 and ZnP_2. The upper limit of zinc according to the Cu10100 standard (Table 2-1) is 1 wtppm. Calculations for OFP copper with 50 wtppm phosphorus at room temperature indicate that zinc should remain in solid solution. The solubility of zinc in copper is high, and zinc-phosphides in OFP copper are unlikely. The first phosphide that will form when increasing the phosphorus content is Cu_3P.

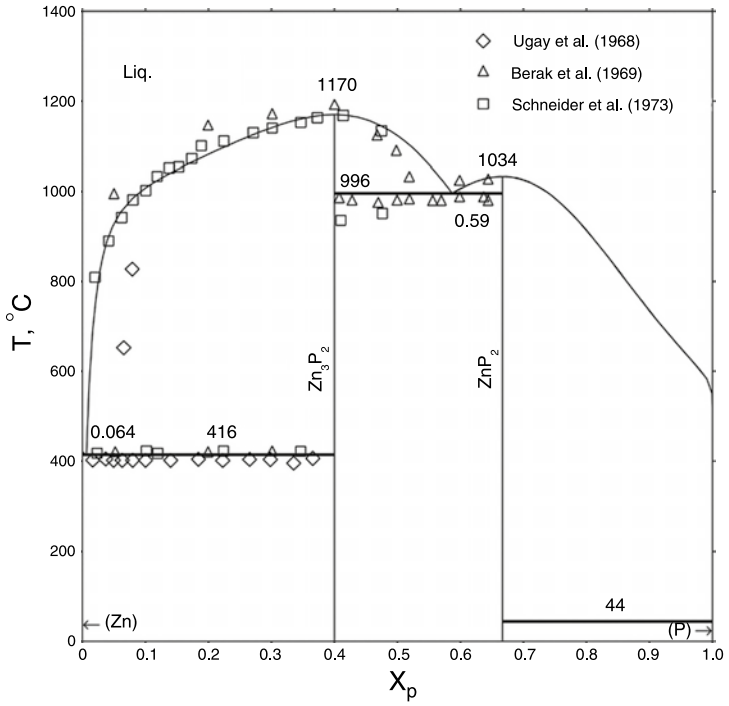

Designation, and typical composition[1]		Space group[1]
Zn	~0 wt% P	$P6_3/mmc$
β-Zn_3P_2 (HT)	~24 wt% P	$Im\bar{3}m$
α-Zn_3P_2 (LT)	~24 wt% P	$P4_2/nmc$
β-ZnP_2 (HT)	~48.7 wt% P	$P2_1/c$
α-ZnP_2 (LT)	~48.7 wt% P	$P4_1\,2_1\,2$
P (Red)	~100 wt% P	–

[1] Data taken from Okamoto (2011).

Figure A-17. *Zn-P phase diagram according to Tu et al. (2009). Phosphides and their crystal structure is taken from Okamoto (2011).*

A2.3 Cu-P-Mn

The P-Mn binary has been evaluated by Miettinen and Vassilev (2014c) as a part of an evaluation of the ternary Fe-Mn-P system. Four phosphides exists, Mn_3P, Mn_2P, MnP, and Mn_3P_2. The manganese-rich part of the Mn-P system is calculated and presented in Figure A-18. The Mn_3P phosphide shares the same stoichiometry as Cu_3P, but they have different crystal structures. The Mn_3P has similar structure as Ni_3P and Fe_3P phosphides. Nowotny and Henglein (1948) have evaluated the miscibility of different phosphides. Only minor dissolution of manganese was found in the Cu_3P phosphide.

The C10100 standard allows for 0.5 wtppm manganese (Table 2-1). The solubility of manganese in copper is high (Section A1.3). Combining the binary descriptions for Cu-P (Noda et al. 2009), Mn-P (Miettinen and Vassilev 2014c), and Cu-Mn (Miettinen 2003), makes is possible to calculate equilibria for the Cu-P-Mn ternary. At room temperature manganese will remain in solid solution. The first forming phosphide when raising the phosphorus content is Cu_3P.

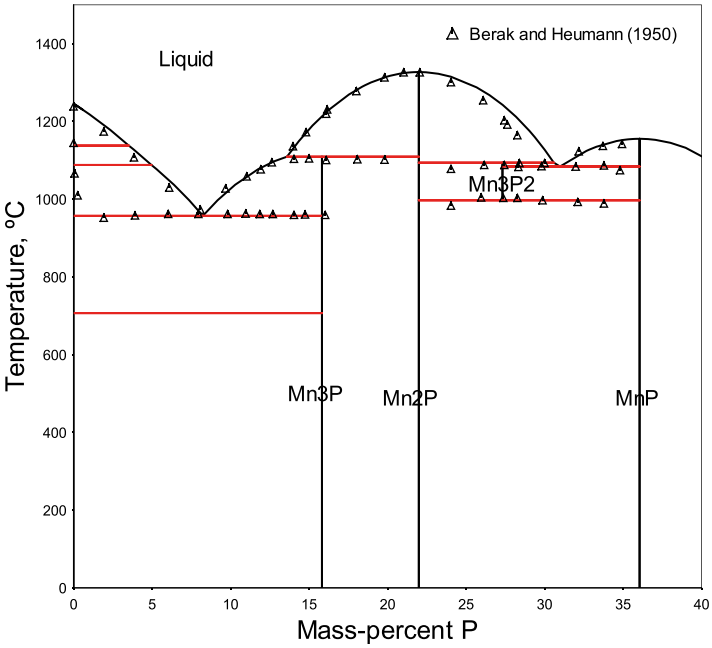

Designation, and typical composition[1]		Space group[1]
α-Mn	~0 wt% P	*cI*58
Mn_3P	~16 wt% P	$I\bar{4}$
Mn_2P	~22 wt% P	$P\bar{6}2m$
Mn_3P_2	~27 wt% P	
MnP	~36.1 wt% P	*Pnma*
P	~100 wt% P	

[1] Data taken from Berak and Heumann (1950).

Figure A-18. *Calculated Mn-rich part of the Mn-P binary system using the parameters by Miettinen and Vassilev (2014c). Experimental data is taken from review by Berak and Heumann (1950).*

A2.4 Cu-P-Fe

The ternary system Cu-P-Fe has been evaluated by Miettinen and Vassilev (2014b). The ternary evaluation was based on the following binaries: Fe-Cu system by Chen and Jin (1995), Cu-P system by Miettinen (2001), and Fe-P system by Miettinen and Vassilev (2014b). The Cu-Fe binary diagram has been calculated and was presented in Figure A-4. A limitation in the work by Miettinen and Vassilev was that the used Fe-P binary did not cover all phosphides, and were limited to up to 40 at% of phosphorus. For this reason, this ternary description will not be used. Instead the work by Ohtani et al. (2006) will be used. They evaluated the whole binary Fe-P binary system. The calculated binary system is presented in Figure A-19. The phosphorus side should be interpreted with care due to lack of experimental data. Some of the data was from higher ordered system, such as Fe-Ti-P. However, all phosphides have quite similar stability.

Calculation for Cu-P-Fe system has been made by combining the three binaries: Fe-P (Ohtani et al. 2006), Cu-Fe (Chen and Jin 1995), and Cu-P (Noda et al. 2009). Following the standard C10100 (Table 2-1), a maximum of 10 wtppm iron is used in calculation together with 50 wtppm phosphorus. Iron has a low solubility in copper and is expected to precipitate. The presence of phosphorus yields FeP_2 as the stable phosphide. FeP_2 is calculated as the most stable phosphide, followed by FeP, Fe_2P, and Fe_3P. All these phosphides have similar stability.

A minor solubility of iron in copper phosphides, and copper in iron phosphides has been reported, but this is not included in the present analysis (Nowotny and Henglein 1948).

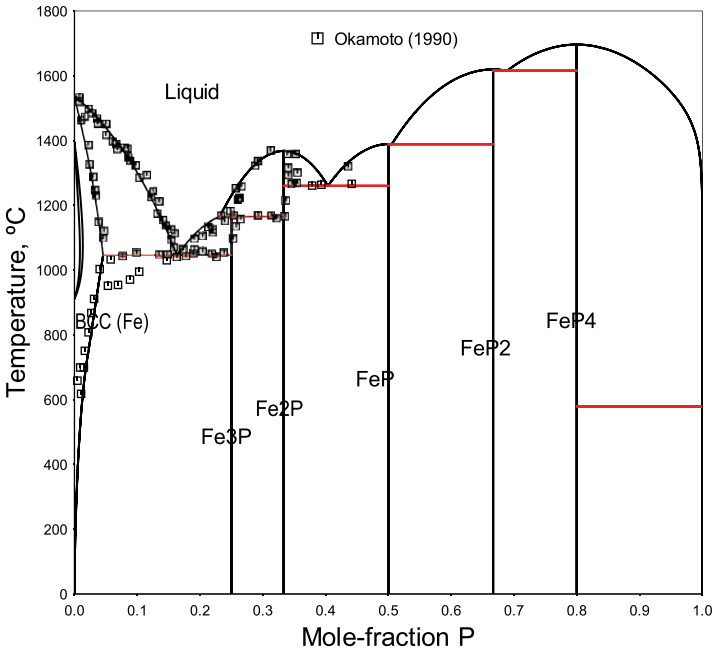

Designation, and typical composition[1]		Space group[1]
α-Fe	0–3 wt% P	$Im\bar{3}m$
γ-Fe	0–3 wt% P	$Fm\bar{3}m$
Fe_3P	~16 wt% P	$I4$
Fe_2P	~22 wt% P	$P\bar{6}2m$
FeP	~36 wt% P	$Pna2_1$
FeP_2	~52 wt% P	$Pnnm$
FeP_4	~69 wt% P	$P2_1/c$
P (red)	~100 wt% P	

[1] Data taken from Okamoto (1990b).

Figure A-19. *Calculated Fe-P binary system using the parameters by Ohtani et al. (2006). Experimental data is taken from Okamoto (1990b), who summarised experimental data from five different references.*

A2.5 Cu-P-Ni

The nickel-rich part of the Ni-P system has been evaluated many times in the past. The most recent one is the evaluation by Miettinen and Vassilev (2015), including phosphorus contents up to 40 at% phosphorus. Some additional experimental data has been produced by Schmetterer et al. (2009), including phosphides NiP_2 and NiP_3 as well. The nickel side of the Ni-P binary system has been calculated, and presented in Figure A-20. Experimental data is taken from Lee and Nash (1991).

Calculations for Cu-P-Ni system, using the binaries Cu-Ni (An Mey 1992), Cu-P (Noda et al. 2009), and Ni-P (Miettinen and Vassilev) has been made. According to the C10100 standard, 10 wtppm of nickel is allowed. Equilibrium calculations for copper with 10 wtppm nickel and 50 wtppm phosphorus yields Ni_2P as stable phosphide at room temperature.

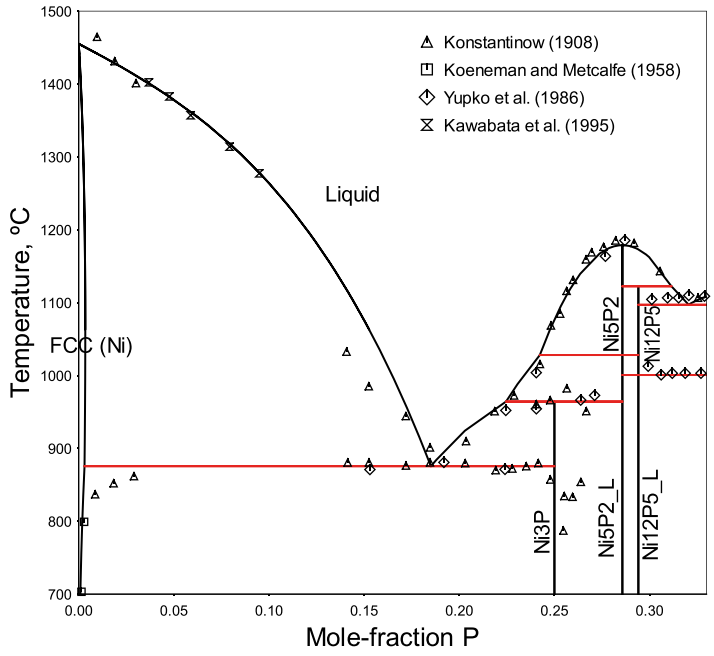

Designation, and typical composition[1]		Space group[1]
Ni	0–0.17 wt% P	$Fm\bar{3}m$
Ni_3P	~15 wt% P	$I4$
Ni_5P_2	~17.5 wt% P	
Ni_5P_2 (LT)	~17.5 wt% P	$P\bar{3}$
$Ni_{12}P_5$	~18 wt% P	
$Ni_{12}P_5$ (LT)	~18 wt% P	$I4/m$
Ni_2P	~21 wt% P	$P\bar{6}2m$
Ni_5P_4	~30 wt% P	$P6_3mc$
NiP	~34.5 wt% P	$Pcba$
NiP_2	~51.4 wt% P	$C2/c$
NiP_3	~61 wt% P	$Im\bar{3}$
P (red)	~100 wt% P	

[1] Data taken from Lee and Nash (1991).

Figure A-20. *Calculated nickel side of Ni-P binary system using the parameters by Miettinen and Vassilev (2015). Experimental data is taken from Lee and Nash (1991).*

A2.6 Cu-P-Sb

The P-Sb system contains no intermediate phases, and the only solution phase included is the liquid. The P-Sb system has been assessed by Ansara et al. (1994). No solid solution was modelled in the crystalline phases, and the whole system was modelled with a single interaction parameter for the liquid.

Calculations for Cu-P-Sb system, using the binaries Cu-Sb (Liu et al. 2000), Cu-P (Noda et al. 2009), and Sb-P (Ansara et al. 1994) has been made. The C10100 standard allows for 4 wtppm of antimony. This is close to the solubility limit at room-temperature, which is extrapolated down to 11 wtppm. No stable antimony phosphides exist, and antimony will remain in solid solution for copper with low concentration of antimony.

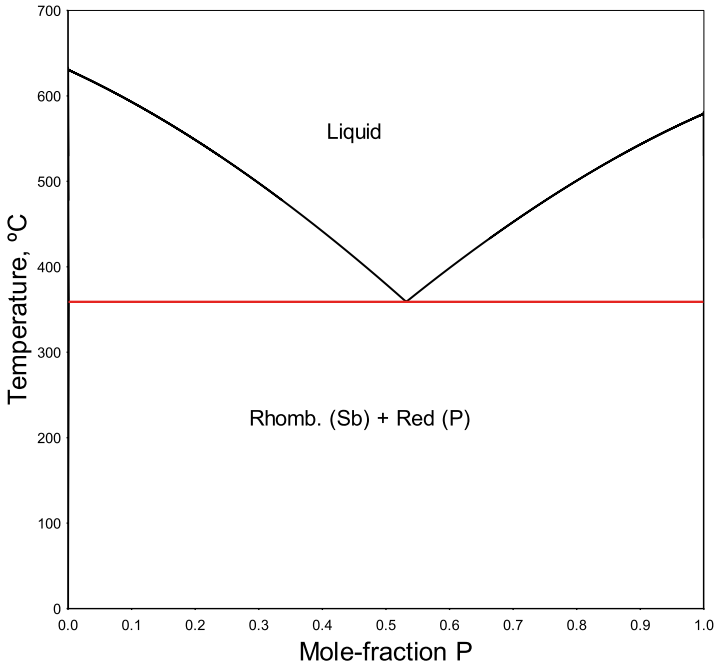

Designation, and typical composition		Space group
Sb (rhomb.)	~0 wt% P	$R\bar{3}m$
P (red)	~100 wt% P	

Figure A-21. *Calculated Sb-P binary according to Ansara et al. (1994).*

A2.7 Cu-P-Sn

Two ternary evaluations of the Cu-P-Sn system have been made, by Miettinen (2001) and by Hino et al. (2011). Hino et al. used the Cu-Sn description by Li et al. (2013). In this work the binary description by Wang et al. (2011) has been used. The differences are minor and for calculations for Cu-P-Sn system the following binaries will be used: Cu-Sn (Wang et al. 2011), Cu-P (Noda et al. 2009), and P-Sn (Hino et al. 2011).

Making calculations at room temperature for 50 wtppm phosphorus and 2 wtppm tin gives both elements in solid solution. The tin-phosphides are not stable enough to precipitate and the first forming phosphide when raising the phosphorus content is Cu_3P.

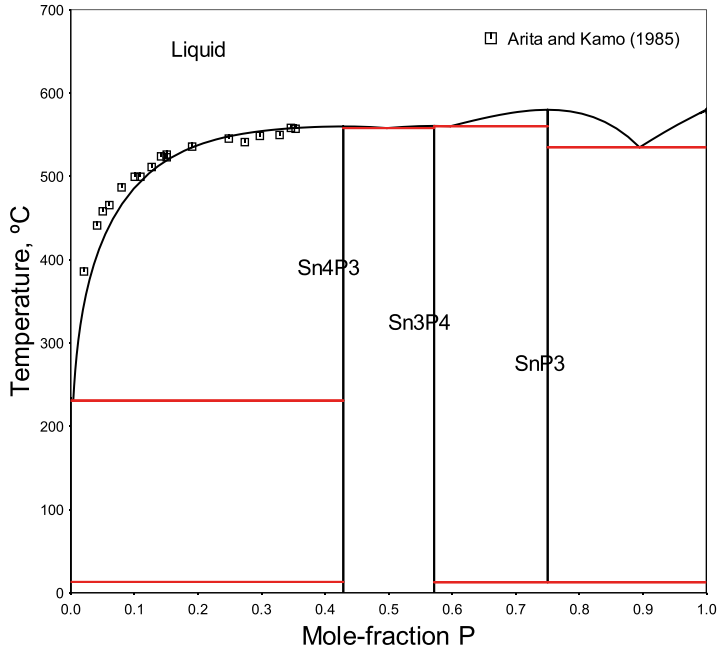

Designation, and typical composition		Space group
Sn (β)	~0 wt% P	I4_1/amd
Sn_4P_3	16.4 wt% P	R3$\bar{}$m 1
Sn_3P_4	25.8 wt% P	R3$\bar{}$m 2
SnP_3	44 wt% P	R3$\bar{}$m 3
P (red)	~100 wt% P	

[1] Data taken from Olofsson (1970).
[2] Data taken from Zaikina et al. (2008).
[3] Data taken from Gullman and Olofsson (1972).

Figure A-22. *Calculated Sn-P binary system using the parameters by Hino et al. (2011). Experimental data is taken from Arita and Kamo (1985).*

A2.8 Cu-P-Pb

Few experimental studies of the P-Pb system exist. Citing an older work, Hansen and Anderko (1958), mention that there exists no reliable information for the P-Pb system. A newer review by Predel (1998), mention the possible stability of a Pb_6P compound. Since no reliable information on the stability of lead phosphides exists in the literature they cannot be included in calculations. Any lead phosphides will therefore not be expected to be stable, and it is expected that lead will precipitate on its own in OFP copper, following the Cu-Pb binary in Section A1.8.

A2.9 Cu-P-Bi

According to Hansen and Anderko (1958), no direct or indirect methods have successfully produced any bismuth phosphides with certainty. The same conclusion is made by a more recent review by Predel (1992) as well. Some more recent reports have indicated the existence of a bismuth phosphide (Carmalt et al. 1994), although it appears to be difficult to produce due to a low stability. The low stability of this possible existing bismuth phosphide makes it reasonable to assume that it has a minor influence on phase equilibria of OFP copper. Calculations for Cu-P-Bi system will therefore follow the binary evaluations, giving phosphorus in solid solution and bismuth precipitating as its own rhombohedral phase (Section A1.9).

A2.10 Cu-P-B

No thermodynamic evaluation of phase diagram data of P-B system has been found in the literature. Compounds belonging to this alloying system have been reported in the literature. Following Predel (1992), stable phases are rhombohedral $B_{13}P_2$, cubic BP, and hexagonal BP. In Wagman et al. (1982) thermochemical data with the heat of formation at 298.15K has been reported as −79 kJ/mol formula unit of BP and −167 kJ/mol formula unit of $B_{13}P_2$.

Combining Cu-B (Wang et al. 2009), with Cu-P (Noda et al. 2009), and the reported heat of formation of BP and $B_{13}P_2$ compounds at 298.15K, makes it possible to calculate the influence of these borides. Using 50 ppm P and 1 ppm B gives phosphorus in solid solution and boron as rhombohedral boron. The first forming phosphide when increasing the phosphorus content is the copper phosphide Cu_3P.

A2.11 Cu-P-Ag

No evaluation of the P-Ag binary system is found in the literature. In an older review of the Ag-P system, like the work by Hansen and Anderko (1958), two phosphides have been reported as stable: AgP_2 and AgP_3. In a later review, by Karakaya and Thompson (1988), it is stated that the phosphide AgP_3 is an erroneous reference to the compound Ag_3P_{11}. The ternary Cu-P-Ag system has been experimentally reviewed by Chang et al. (1977). Very little solid solution between the three elements is reported.

The thermochemical data for the phosphides AgP_2 and AgP_3 have been tabulated by Barin (1995). The Gibbs energy of formation per formula unit is AgP_2 −43.3 kJ/mol, and AgP_3 −69.5 kJ/mol. Data on the stability of these phosphides will be used to calculate equilibria at room-temperature, together with the Cu-Ag binary (Moon et al. 2000), and Cu-P binary (Noda et al. 2009). Calculations based on 25 wtppm of silver and 50 wtppm of phosphorus yields metallic silver in a copper matrix with phosphorus in solid solution. The first forming phosphide is Cu_3P when increasing the phosphorus content.

A2.12 Cu-P-Cd

Several different cadmium phosphides have been reported in the literature, as listed in Table A-1. According to a review by Schlesinger (2002) on binary phosphides there exist thermochemical data for some of these phosphides. However, due to the considerable scatter in reported data the values were not considered as reliable. The Gibbs energy of formation for the following reaction $3Cd+0.5P_4(g) = Cd_3P_2$, is estimated as −47.1 to −226.2 kJ/mol.

The possible influence of cadmium phosphides in OFP copper has been investigated. By combining the binaries Cu-P (Noda et al. 2009) and Cu-Cd (Chen et al. 2010) and the estimated stability of Cd_3P_2 based on the reported Gibbs energies of formation, calculations can be made for the Cu-P-Cd system. The calculations indicate that even the most extreme reported Gibbs energy is not enough to make it stable for OFP copper with 50 wtppm phosphorus and 1 wtppm cadmium. Cadmium prefers to stay in solid solution, and possibly precipitate as Cu_2Cd (Section A1.12).

Table A-1. Stable Cd-P compounds, according to Okamoto (1990a).

Designation, and typical composition		Space group
Cd	~0 wt% P	$P6_3/mmc$
Cd_3P_2	16	$P4_2/nmc$
Cd_6P_7	24.3 wt% P	
Cd_7P_{10}	24.3 wt% P	$Fdd2$
β CdP_2	35.6 wt% P	$P4_32_12$
α CdP_2	35.6 wt% P	$Pna2_1$
CdP_4	52.4 wt% P	$P2_1/c$

A2.13 Cu-P-Hg

According to Schlesinger (2002) no mercury phosphides are known. The same conclusion is made in a more recent review of experimental data belonging to P-Hg system, by Gumiński 2005). Due to the limited interaction between mercury and phosphorus, these two elements will follow their copper binary. This means that mercury might precipitate as metallic mercury or Cu_7Hg_6 compound at low temperature.

A2.14 Cu-P-Se

Reported selenium phosphides are P_4Se_4, P_4Se_3, and P_4 Se_5, according to Schlesinger (2002). No reported enthalpy of formation or Gibbs energy of formation for these compounds has been found. The phosphorus part of the P-Se phase diagram can be found in handbook (Predel 1998). It shows the existence of the P_4Se_3 selenide that has a relative low melting point. A related binary system, the P-S system, is more studied than P-Se. In similarity with selenium also sulphur has a very low solubility in metallic copper. It forms many different phosphides of similar stoichiometry, but all are of low stability. It is reasonable to believe that selenium will follow sulphur, by reacting with copper rather than phosphorus.

A2.15 Cu-P-Te

Reported tellurium phosphide is PTe, according to a review of the experimental thermodynamic data belonging to this binary system (Okamoto 2010). This phosphide only form when phosphorus of white structure and tellurium is combined. The phosphide is stable up to 110 °C when it melts. When using the more stable red and black phosphorus, the phosphide will not form. No enthalpy or Gibbs energy of formation for this phosphide has been reported in the literature. However, due to the low stability of this low-melting phosphide, and the fact that it is not stable when more stable allotropes of phosphorus is present, this tellurium phosphide will not be of interest for OFP copper. Calculations for OFP copper will follow the binary evaluations Cu-P and Cu-Te (Section A1.15), which indicated a very low solubility of tellurium in copper, and any phosphorus addition will not change this. Tellurium therefore shows a similar appearance as both selenium and sulphur, by having a low solubility in metallic copper and forming less stable phosphides with phosphorus.

Arkitektkopia AB, Bromma, 2018

SKB is responsible for managing spent nuclear fuel and radioactive waste produced by the Swedish nuclear power plants such that man and the environment are protected in the near and distant future.

skb.se